NASA Contractor Report 178171

Evaluation of Pactruss Design Characteristics Critical to Space Station Primary Structure

John M. Hedgepeth
Astro Aerospace Corporation
Carpinteria, California

Prepared for
Langley Research Center
under Contract NAS1-17536, Task 6

20 February 1987

National Aeronautics and Space Administration

Langley Research Center
Hampton, Virginia 23665-5225

NASA Contractor Report 178171

Evaluation of Pactruss Design Characteristics Critical to Space Station Primary Structure

John M. Hedgepeth
Astro Aerospace Corporation
Carpinteria, California

Prepared for
Langley Research Center
under Contract NAS1-17536, Task 6

20 February 1987

National Aeronautics and
Space Administration

Langley Research Center
Hampton, Virginia 23665-5225

TABLE OF CONTENTS

LIST OF FIGURES

SECTION 1
INTRODUCTION

The Pactruss concept has been described and examined in Reference 1. In Reference 2, the Pactruss is established as a candidate for the primary structural truss on the Space Station. Its attractiveness stems from the ability to deploy a large-sized truss (15-foot cells) from a compact package. The deployment is strongly self-synchronized; thus, the deployment can be actuated and controlled by only a few (perhaps only one) active drivers, with consequent greatly reduced cost and weight of the deployment system. Past examination has also shown that the Pactruss can include significant variations in its designs so as to allow for pre-installed utilities, integration with an MRMS, and choices of deployed geometrics. It can be used as a beam (see Figure 1), an area truss (Figure 2) or a combination of the two.

In order that Space Station planners can be provided with the proper information on which decisions can be reached about the type and size of structure to be used on Space Station, more detailed examination is reported herein on those aspects of Pactruss that are critical to its use.

SECTION 2
INTERNAL STIFFNESS OF TRUSSES

If the members in a redundant truss are not of the correct length because of thermal strains, fabrication errors, or deployment or assembly kinematics, deleterious internal loads may result. During deployment or assembly, the mechanisms, joints and tools available must be forceful enough to overcome any resistance from mismatching geometry. The estimation of the magnitude of the loads due to mismatch is clearly necessary to establish the requirements for deployment and assembly devices.

Of course, the mismatch loads are dependent on the stiffness of the redundant structure bounding the misfitting member. If the surrounding structure is rigid, all of the mismatch will have to be absorbed by the member itself. Such an assumption could be useful to get a worst-case estimate, but may yield unrealistically large loads. More useful results can be obtained by estimating the internal stiffness of several generic truss configurations.

Cube Truss

Consider the cube truss shown in Figure 3. Let the base of the cube be fixed and loads applied at the upper corners as shown. The diagonal and longeron loads shown in the figure are easily determined by statics. The resulting strain energy is

$$S.E. = \frac{1}{2}\left[2\ell\,\frac{(\sqrt{2}\,P)^2}{EA_\ell} + 4\sqrt{2}\,\ell\,\frac{P^2}{EA_d}\right]$$

where EA_ℓ and EA_d are the extensional stiffnesses of the longerons and diagonals, respectively. The compliance is determined by differentiating with respect to P. This gives

$$C_{truss} = C_{diag}\,(4 + 2\sqrt{2}\,EA_d/EA_\ell) \qquad (1)$$

where

$$C_{diag} = \frac{\sqrt{2}\,\ell}{EA_d} \tag{2}$$

is the axial compliance of a diagonal.

Thus, if the longeron and diagonals have the same stiffness per unit length, the compliance of the truss is almost seven times that of the diagonal. Even if the longerons are much stiffer than the diagonals, the truss compliance is four times that of the diagonal.

Square Lattice With Parallel Diagonals

Another pertinent truss configuration is shown in Figure 4. This is a planar square lattice with parallel diagonals. Useful estimates can be obtained by letting the lattice be infinite in extent and assuming a central member to be preloaded.

With the numbering system and nomenclature shown in Figure 4, the equilibrium and load-displacement relations are

$$\left.\begin{aligned} p(m,n) - p(m-1,n) + \frac{\sqrt{2}}{2}\,[t(m,n) - t(m-1,n-1)] &= 0 \\ q(m,n) - q(m,n-1) + \frac{\sqrt{2}}{2}\,[t(m,n) - t(m-1,n-1)] &= 0 \end{aligned}\right\} \tag{3}$$

$$\left.\begin{aligned} p(m,n) &= \frac{EA_\ell}{\ell}\,[u(m+1,n) - u(m,n)] + p_o(m,n) \\ q(m,n) &= \frac{EA_\ell}{\ell}\,[v(m,n+1) - v(m,n)] + q_o(m,n) \\ t(m,n) &= \frac{EA_\ell}{\ell}\,[u(m+1,n+1) - u(m,n) + v(m+1,n+1) - v(m,n)] + t_o(m,n) \end{aligned}\right\} \tag{4}$$

The preloads $p_o(m,n)$, $q_o(m,n)$ and $t_o(m,n)$ are the loads that would appear in the lattice if the deflections were restrained to be zero.

In order to solve these equations, it is appropriate to use double Fourier transforms as was done, for example, in Reference 3.

Thus we define transform pairs for each variable. For example, the transform of the load p(m,n) is

$$\bar{p}(x,y) = \sum_{m=-\infty}^{\infty} \sum_{n=-\infty}^{\infty} p(m,n)e^{-imx}e^{-iny} \tag{5}$$

and the inverse tranform is

$$p(m,n) = \frac{1}{(2\pi)^2} \int_{-\pi}^{\pi} \int_{-\pi}^{\pi} \bar{p}(x,y)e^{imx}e^{iny}dx\,dy \tag{6}$$

Taking transforms of the load-displacement relations [eq. (4)] yields

$$\bar{p} = 2i \frac{EA_\ell}{\ell} e^{ix/2} \sin\frac{x}{2}\ \bar{u} + \bar{p}_o$$

$$\bar{q} = 2i \frac{EA_\ell}{\ell} e^{in/2} \sin\frac{y}{2}\ \bar{v} + \bar{q}_o$$

$$t = i \frac{EA_d}{\ell} e^{i(x+y)/2} \sin\frac{x+y}{2}\ (\bar{u}+\bar{v}) + \bar{t}_o$$

Eliminating $\bar{u}$ and $\bar{v}$ yields

$$\bar{t}-\bar{t}_o = \frac{1}{2}\frac{EA}{EA_\ell}\sin\frac{x+y}{2}\left[\frac{e^{iy/2}}{\sin x/2}(\bar{p}-\bar{p}_o) + \frac{e^{ix/2}}{\sin y/2}(\bar{q}-\bar{q}_o)\right] \tag{7}$$

The transforms of the equilibrium relations [eq. (3)] are

$$\left.\begin{aligned} e^{iy/2}\sin\frac{x}{2}\bar{p} + \frac{\sqrt{2}}{2}\sin\frac{x+y}{2}\bar{t} &= 0 \\ e^{iy/2}\sin\frac{y}{2}\bar{q} + \frac{\sqrt{2}}{2}\sin\frac{x+y}{2}\bar{t} &= 0 \end{aligned}\right\} \tag{8}$$

Equations (7) and (8) constitute three equations in the three unknown load transforms. Each load can readily be obtained in terms of the preloads. for the present purpose, only the relationship of each load with its preload is required. Solving gives

$$\frac{\bar{t}}{\bar{t}_o} = \frac{\sin^2\frac{x}{2}\sin^2\frac{y}{2}}{\sin^2\frac{x}{2}\sin^2\frac{y}{2} + \frac{\sqrt{2}}{2}\frac{EA_d}{EA_\ell}\left(\sin^2\frac{x}{2}+\sin^2\frac{y}{2}\right)\sin^2\frac{x+y}{2}}, \quad \bar{p}_o = \bar{q}_o = 0 \tag{9}$$

$$\frac{\bar{p}}{\bar{p}_o} = \frac{\frac{\sqrt{2}}{4}\frac{EA_d}{EA_\ell}\sin^2\frac{y}{2}\sin^2\frac{x+y}{2}}{\sin^2\frac{x}{2}\sin^2\frac{y}{2} + \frac{\sqrt{2}}{2}\frac{EA_d}{EA_\ell}\left(\sin^2\frac{x}{2}+\sin^2\frac{y}{2}\right)\sin^2\frac{x+y}{2}}, \quad \bar{t}_o = \bar{q}_o = 0 \tag{10}$$

Assume that each preload results in a prestrain ϵ_o in the $m = 0$, $n = 0$ member. Thus, for example,

$$t_o = -EA_d\epsilon_o \quad , m,n = 0$$

$$= 0 \qquad , \text{otherwise}$$

Then

$$\bar{t} = -EA_d\epsilon_o$$

The resulting load in the (0,0) diagonal is then

$$t(0,0) = t_o(0,0)\,\frac{1}{(2\pi)^2}\int_{-\pi}^{\pi}\int_{-\pi}^{\pi}\frac{\bar{t}}{\bar{t}_o}\,dx\,dy \tag{11}$$

In terms of the previous compliance notation, the resulting load could also be determined as follows

$$T(0,0) = -\frac{\sqrt{2}\,\ell\epsilon_o}{C_{truss} + C_{diag}}$$

$$= -\frac{EA_d\epsilon_o}{1 + \dfrac{C_{truss}}{C_{diag}}}$$

Thus

$$\frac{C_{truss}}{C_{diag}} = \frac{t_o(0,0)}{t(0,0)} - 1 \tag{12}$$

In a similar way, the compliance ratio for the longerons can be found to be

$$\frac{C_{truss}}{C_{long}} = \frac{p_o(0,0)}{p(0,0)} - 1 \tag{13}$$

where

$$\frac{p(0,0)}{p_o(0,0)} = \frac{1}{(2\pi)^2} \int_{-\pi}^{\pi} \int_{-\pi}^{\pi} \frac{\bar{p}}{\bar{p}_o} \, dx \, dy \tag{14}$$

Numerical results are obtained subsequently.

Square Lattice With Diamond Diagonals

An alternative arrangement of diagonals is shown in Figure 5. The equilibrium and load-displacement relations are

$$p(m,n) - p(m-1,n-1) + \frac{\sqrt{2}}{2} [t(m,n) - t(m,n-1) + s(m,n) - s(m-1,n)] = 0$$

$$q(m,n) - q(m+1,n-1) + \frac{\sqrt{2}}{2} [t(m,n-1) - t(m,n-1) - s(m-1,n)] = 0$$

$$p(m,n) - p_o(m,n) = \frac{EA_\ell}{2\ell} [u(m+1,n+1) - u(m,n)]$$

$$q(m,n) - q_o(m,n) = \frac{EA_\ell}{2\ell} [v(m-1,n+1) - v(m,n)]$$

$$t(m,n) - t_o(m,n) = \frac{EA_d}{2\ell} [u(m,n+1) - u(m,n) + v(m,n+1) - v(m,n)]$$

$$s(m,n) - s_o(m,n) = \frac{EA_d}{2\ell} [u(m+1,n) - u(m,n) - v(m+1,n) + v(m,n)]$$

with the notation of Figure 5. Note that only the nodes to which diagonals are attached are numbered; there is no load change across the others.

Going through the same procedure as with the preceding diagonal arrangement yields the results for compliance in the same form as equations (12) and (14) with the transformed load ratios given by

$$\frac{\bar{t}}{\bar{t}_o} = \frac{N_t}{D} \tag{15}$$

and

$$\frac{\bar{p}}{\bar{p}_o} = \frac{N_p}{D} \tag{16}$$

where

$$\left.\begin{aligned} N_p &= -\frac{\sqrt{2}}{2}\frac{EA_d}{EA_\ell}\sin^2\frac{x-y}{2}\left(\sin^2\frac{x}{2}+\sin^2\frac{y}{2}\right)+2\left(\frac{EA_d}{EA_\ell}\right)^2\sin^2\frac{x}{2}\sin^2\frac{y}{2} \\ N_t &= \sin^2\frac{x+y}{2}\sin^2\frac{x-y}{2}+\frac{\sqrt{2}}{2}\frac{EA_d}{EA_\ell}\left(\sin^2\frac{x+y}{2}+\sin^2\frac{x-y}{2}\right)\sin^2\frac{x}{2} \\ D &= \sin^2\frac{x+y}{2}\sin^2\frac{x-y}{2}+-\frac{\sqrt{2}}{2}\frac{EA_d}{EA_\ell}\left(\sin^2\frac{x+y}{2}+\sin^2\frac{x-y}{2}\right) \\ &\quad \left(\sin^2\frac{x}{2}+\sin^2\frac{y}{2}\right)+2\left(\frac{EA_d}{EA_\ell}\right)^2\sin^2\frac{x}{2}\sin^2\frac{y}{2} \end{aligned}\right\} \tag{17}$$

SECTION 3
NUMERICAL RESULTS

The ratio of compliance of the truss to that of the member under consideration is shown in Figure 6 for a number of examples. The ratios are shown as a function of the ratio between the stiffness per unit length of the diagonals and that of the longerons. The curve for the cube truss is determined from equation(1); those for the lattices are calculated by evaluating the integrals in equations (11) and (14) with the appropriate integrands. Double numerical integration with 50 by 50 elemental boxes in each quadrant is employed. The integral is evaluated at the center of each box and multiplied by the area of the box. Summing yields the approximate integral.

Also shown in Figure 6 are results for two other configurations in which the diagonal and longeron extensional stiffnesses are equal. One is for an equilateral-triangle lattice (isogrid) as obtained in Reference 3. The other is for the longeron mismatch at the middle of a 16-bay truss beam, calculated by finite-element analysis by John T. Dorsey of NASA Langley Research Center. The spread band represents the limits for two beam diagonal arrangements and two longeron locations.

Examining the results in Figure 6 yields the conclusion that conservative estimates of loads in members due to local mismatch will be reached if the compliance ratio of five is assumed for a beam-like structure. For an area truss, a compliance ratio of unity should be assumed.

SECTION 4
LOADS IN A DEPLOYING DIAGONAL MEMBER

When a folding diagonal is nearing full deployment in a redundant truss structure, it must go "over center" because of the longer distance between hinge lines than between the butted surfaces. In addition, the length available for the deployed diagonal may be too large or too small because of fabrication imperfections or thermal strains. Consequently, internal hinge moments are needed to drive the deployment to full completion. The purpose of this section is to evaluate the necessary hinge moments in order to support proper hinge design.

A partly deployed folding strut is shown in Figure 7. Note that the undistorted length of each half strut is $\ell/2$ and the center hinge is offset from the centerline by the distance e. The ends are pivoted at the centerline. At each end there are deployment resisting moments, M_f. (These presumably arise from friction and the bending stiffness of any preintegrated electrical cables.) The moment M_h at the center hinge drives the assembly toward full deployment, and the compressive force P pushes the ends together.

Let y be the displacement of the centerline of the strut from the fully deployed state. Equating internal and external moments yields

$$EIy'' + Py = -M_f \tag{18}$$

where EI is the bending stiffness of the strut. The solution for y is

$$y = -\frac{M_f}{P}\left[1 - \left(\cos\frac{\lambda x}{\ell}\right) + \left(\frac{\theta\ell}{2\sin\lambda/2} + \frac{M_f}{P}\,\frac{1-\cos\lambda/2}{\sin\lambda/2}\right)\sin\frac{\lambda x}{\ell}\right] \tag{19}$$

where x is measured form the left end,

$$\lambda^2 = \frac{P\ell^2}{EI} \tag{20}$$

and θ is the slope of the line joining the ends of the half strut.

Treat the half strut as a free body. Then

$$M_h = M_f + P\,\theta\ell/2 - Pe$$

Let the leftward movement of the center hingeline be δ. Then

$$\delta = \frac{P\ell}{2EA} + \frac{1}{2}\int_0^{\ell/2} (y')^2\,dx - ey'\,\frac{\ell}{2}$$

Substituting for y, integrating, and combining gives

$$\delta = \frac{\ell}{2}\,[A - B\theta + C\theta^2] \tag{21}$$

where

$$\left.\begin{aligned} A &= \lambda^2\,\frac{\rho^2}{\ell^2} + \frac{2e}{\ell}\,\frac{1-\cos\lambda/2}{\lambda\sin\lambda/2}\,\frac{M_f\ell}{EI} + \frac{1}{4}\,\frac{\lambda-2\sin\lambda/2}{\lambda^3\cos^2\lambda/4}\left(\frac{M_f\ell}{EI}\right)^2 \\ B &= 2\,\frac{e}{\ell}\,\frac{\lambda\cos\lambda/2}{2\sin\lambda/2} - \frac{1}{8}\,\frac{\lambda - 2\sin\lambda/2}{\lambda\cos^2\lambda/4}\,\frac{M_f\ell}{EI} \\ C &= \frac{\lambda^2 + \lambda\sin\lambda}{16\sin^2\lambda/2} \end{aligned}\right\} \tag{22}$$

where

$$\rho^2 = \frac{EI}{EA} \tag{23}$$

If the half strut is in tension, then λ^2 is negative and the trigonometric functions must be replaced with hyperbolic ones.

Let $\gamma = \sqrt{-\lambda^2}$. In that case

$$\left.\begin{aligned} A &= -\gamma^2 \frac{\rho^2}{\ell^2} + \frac{2e}{\ell} + \frac{\cosh \gamma/2 - 1}{\gamma \sinh \gamma/2} \frac{M_f \ell}{EI} + \frac{1}{4} \frac{2 \sinh \gamma/2 - \gamma}{\gamma^3 \cosh^2 \gamma/4} \left(\frac{M_f}{EI}\right)^2 \\ B &= \frac{2e}{\ell} \frac{\gamma \cosh \gamma/2}{\gamma \sinh \gamma/2} + \frac{1}{8} \frac{2 \sinh \gamma/2 - \gamma}{\gamma \cosh^2 \gamma/4} \frac{M_f \ell}{EI} \\ C &= \frac{\gamma^2 + \gamma \sinh \gamma}{16 \sinh^2 \gamma/2} \end{aligned}\right\} \quad (24)$$

Note the the center hinge moment in nondimensional form is

$$\frac{M_h \ell}{EI} = \frac{M_f \ell}{EI} + \frac{\lambda^2}{2} \left(\theta - 2 \frac{e}{\ell}\right) \quad (25)$$

Also of interest is the hinge opening angle α which is twice the center slope. Thus

$$\alpha = \frac{\lambda \cos \lambda/2}{\sin \lambda/2} \theta - 2 \frac{1 - \cos 1/2}{\lambda \sin \lambda/2} \frac{M_f \ell}{EI} \quad (26)$$

Of course, α must be positive.

The deploying diagonal must fit into the length established by the surrounding truss. Thus the total shortening of the diagonal must be

$$2\delta = \epsilon_0 \ell - P\, C_{truss} \quad (27)$$

where ϵ_0 is the unit shortening of the length available for the diagonal and C_{truss} is the compliance of the truss defined in the preceding section.

Combining equations (21) and (27) gives

$$C\theta^2 - B\theta + A + \lambda^2 \frac{\rho^2}{\ell^2} \frac{C_{truss}}{C_{diag}} = \epsilon_0 \qquad (28)$$

which can be solved for θ for various values of end load P.

Example results are shown in Figure 8, which applies to a thin-walled tube with the center hinge located at the outer surface. Thus

$$\rho^2 = d^2/8$$

$$e = d/2$$

The value of d chosen is 0.008 times the length.

The results in Figure 8 are in nondimensional form. Note, for example, that the pin-ended Euler load for the full diagonal would produce

$$\frac{P\ell^2}{EI} = \pi^2$$

As the diagonal straightens (α decreases), the compression load increases to a maximum, then decreases as the diagonal hinge closes. The hinge moment required to cause closure reaches a maximum before the compression load peaks, then decreases and becomes negative as the hinge line passes through the line joining the two ends; the compression load then helps to close the hinge.

The combined effect of the hinge moment and the offset hinge location is to cause the diagonal halves to bend significantly, thereby relieving the compression load as the hinge line approaches the line joining the two ends. The importance of this effect is emphasized by noting that the axial strain without bending relief would otherwise reach $1/2\ (d/\ell)^2$. For a compliance ratio of one, the resulting maximum nondimensional load would be 2.5.

If the length available of the diagonal is less than a diagonal length, then the behavior, as seen in Figure 8, is similar; the magnitudes are greater

but the maximum required hinge moment occurs at about the same angle, which is about one and a half degrees.

The maximum required hinge moment is shown in Figure 9 as a function of the excess diagonal length. The results are shown in dimensional form for proportions and stiffness appropriate to the Space Station. The physical quantities are given in the figure.

The greatest value of excess length considered is 0.025 inches, which is estimated to be large enough to encompass fabrication errors as well as thermal and load straining. Note that the maximum required hinge moment is in the order of several hundred inch-pounds for the "stiff" truss case (compliance ratio = 1) for such an excess length; the effects of a reasonable amount of friction or of moving the hinge axis to the centerline are relatively minor. Fortunately, for the Space Station baseline design, a "soft" truss (compliance ratio of 5) is appropriate. The worst-case required moment is then about 200 inch-pounds.

In order to provide margin, the central diagonal hinges on the Space Station Pactruss should be designed to provide 300 inch-pounds of closing moment at a hinge opening of one and one-half degrees.

SECTION 5
JOINT DESIGN CONCEPTS

The Pactruss has two general types of deployable joints. One is the diagonal mid-hinge; the other is the centered-pin hinge at the ends of all struts. For both types the joints should satisfy the following suggested requirements (see also Reference 2):

1. Less than 0.0005 inch displacement offset (compression-to-tension hysteresis) in order that non-linear effects be acceptably small.
2. Axial compliance less than one microinch per pound in order to avoid significant reduction of overall strut stiffness.
3. Deploy reliably and repeatedly throughout the environmental range.
4. Provide for repair or replacement of struts.
5. Accommodate preinstalled utility lines.
6. Stow compactly.

In addition, the cluster body to which the strut ends join must provide for the preattachment of MRMS interface hardware as well as the post-attachment of payloads and growth structure. The design must provide space not only for the structure but also for pre-installed utility lines.

Strut-End Joints

The centered-pin hinge at the end of each strut must be tight enough to avoid nonlinearity without being too hard to turn. Work on the Deployable Ground Test Beam (deliverable to Langley Research Center) at Astro has shown that it is possible to accomplish this objective. Experimental data are plotted in Figure 10 for a titanium joint with a 0.3125-inch pin with a slip-fit, [Figure 10(a)] and with a 0.0002-inch interference-fit 0.378-inch-diameter pin [Figure-10(b)]. It can be seen that the nonlinearity is nearly eliminated by the tight pin and that the hysteresis is less than 0.0005 inch. The data

also show that the compliance is 1.2 microinches per pound and that the turning moment is five inch-pounds. While much work needs to be done to assure reliability, these initial results are very encouraging.

Repair and replacement in space can be accomplished with powered tools which can attach to an internally-threaded hinge pin and extract it. Reassembly would use expanding tapered pins to produce a zero-displacement, low-compliance joint.

The erection of add-ons can be accommodated by suitable bolt-on adapters which would interface with predrilled and tapped holes in the cluster body.

Mid-Diagonal Joint

In addition to the requirements listed at the beginning of this section, the diagonal knee joint must supply sufficient hinge moment to ensure full straightening of the diagonal. Furthermore, the articulation of 180 degrees requires that either the hinge pin is off-center or that the joint is complex. In the interests of simplicity, an off-center hinge was selected. The preceding section contains an analysis of this approach; it concludes with a requirement of 300 inch-pounds of closing moment for the Space Station design.

It was decided to achieve the needed closing moment by installing a latch which presses the joint faces together at the centerline. In this way, the axial loads in a fully deployed diagonal are carried through the mid-diagonal joint by the flat faces rather than by the hinge pins.

The forces needed for deployment moment can also provide the precompression required to ensure good contact, and hence low compliance, of the faces. Figure 11, taken from Reference 2, shows that a preload of 300 pounds can make the compliance small, even when a 0.005-inch unevenness is assumed.

Two concepts for center-loading latches are shown in Figure 12. The single-stage latch is simpler but requires significant moment in the early deployment stages to compress the driving spring. Toward the end of deployment, the mechanical advantage will magnify the moment and produce a

large torque in the desired direction. The amount of magnification, however, is limited; thus a large spring with a large amount of strain energy is needed.

In order to remedy the deficiencies of the single-stage latch, a second stage was added. Its operation is illustrated in Figure 12(b). Note that the linkage of Figure 12(a) is retained and another force-multiplying linkge drives the retained one. Torsional springs located at pivots 3 and 5 produce the deploying power.

An analysis was made of the kinematics and moment ratios achieved with the two-stage latch for various geometries. A computer program for calculating is included in Appendix A. From numerous trials, the design pivot fully-deployed positions were found as follows (origin is at the hinge with x along the diagonal):

Pivot	x, inches	y, inches
Hinge	0	0
0	0	1.000
1	-0.600	1.000
2	1.500	1.300
3	2.000	2.700
4	2.000	0.700
5	2.500	4.500

The moment magnification ratios for this design are shown in Figure 13. Note that at both pivots, the moment ratio is small for most of the deployment; large disturbimg torques are avoided during the early and mid stages. Near full deployment, the almost-over-center characteristics assert themselves and the moment ratio grows dramatically.

Figure 13(b) is concentrated on the final deployment stage. Also shown are results obtained by assuming that the pivots are mislocated by 0.001 inch in a worst-case fashion. It can be seen that the moment ratio achieved at one and one-half degrees from full deployment (the maximum-required-moment angle from the preceding section) is about ten. Therefore, a total spring torque at pivots 3 and 5 of about 30 inch-pounds is needed. Detailed numerical results are provided in Appendix A.

The conclusion is that the two-stage latch can supply the deployment moment required in a controlled fashion and that it will provide a high level of preload in the deployed joint.

SECTION 6
OVERALL PACTRUSS DEPLOYMENT

The Pactruss concept is most useful when a large amount of structure is deployed simultaneously. This deployment must be controllable and reliable. The problems of reliability are illustrated in Figure 14. The effects of joint resistance, external disturbances, mid-diagonal hinge moments and structural flexibility must be dealt with by deployment actuators located at the cluster joints, controlling the hinge angle at the strut end joints. Without the disturbing effects, it is possible to actuate the deployment from a single point; that is the advantage of the Pactruss concept. The question is how many actuators are required to provide confident control in the real situation.

Providing control with multiple actuators is a straightforward task. One concept is shown in Figure 15. Here the gear-motor-driven arm rotates the longeron away from the vertical. A shaft encoder on each actuator enables a central controller to keep the several actuators synchronized. Also installed is a force sensor which will allow monitoring the deployment. If nonstandard loads occur, then the data will facilitate the fault analysis. Finally, the actuator can be mechanically disconnected if it is at fault, probably by EVA.

Determining how may actuators are required, where to place them, and what are their detailed design criteria will require a high-fidelity analytical simulation as well as experimental investigations. Such a tool will involve dealing with large angles and large displacements, together with structural deformations. The fact that the intended deployment is very gradual (taking, say, 30 minutes) makes dynamic effects negligible, at least for the nominal design case. Nevertheless, the capability needed for quasi-static analysis may be outside of the present state of art.

In order to assess the current capability, the NASTRAN finite-element analysis program was applied by P. Kimbrough of the MacNeal-Schwendler Corporation to an example eight-bay Pactruss beam of Space Station propor-

tions. A considerable amount of difficulty was encountered despite the original perception that the desired quasi-static analysis was straightforward.

In the model, large displacements were included as well as realistic offsets between the hinge joints and the nodal points. Actuation occurred at one joint at an end of the beam and all other hinges were assumed to have a frictional retarding torque. It was found that not all the needed types of elements are available in the large-rotation form and some modeling approximations were required. Convergence was slow and required small steps between iterative episodes. For example, for a step of one inch-pound frictional moment, a time of 21 minutes on a MicroVax/Step was needed.

The conclusion reached in this analysis attempt is that while the detailed tools are not currently available, they can reasonably be expected to be developed without great effort. NASTRAN or other finite-element codes can therefore be expected to provide the capability of at least quasi-static analysis of deploying truss structures.

A capability of testing the deployment of the Pactruss is also needed in both the design and testing phases of the Space Station program. The direct approach will require testing of the entire flight structural package with sufficiently good gravity compensation. In fact, the ground testing may very well establish the number and location of the deployment actuators.

During deployment, various parts of the structure move hundreds of inches relative to each other in all directions. If these motions are not counterbalanced in detail, significant amounts of energy will be needed from the actuators. For example, a bay weighing 120 pounds will absorb 12 inch-pounds of energy in a 0.1-inch vertical motion. If there is one actuator for each ten bays, then it would need to exert 120 inch-pounds of energy. But the actuator will probably need to be limited to 500 inch-pounds of torque in order to avoid overloading the struts. So the design margin is not great.

Perhaps it will be necessary to resort to testing subsections of the structure. Reliability of deployment would be verified with analysis. The importance of a good analytical simulation is further strengthened.

SECTION 7
VERIFICATION TESTING

A verification test plan for the Pactruss was prepared by P. Preiswerk of Astro Aerospace. The approach was to modify a test plan used for verifying the deliverable hardware for a flight project appropriately. The resulting plan is included as Appendix B. Items are summarized below:

Pactruss Tests

Materials, Parts and Subassembly Tests

- Truss member material test
- Truss component tension test
- Motor or actuator qualification/acceptance test
- Acceptance test of other electromechanical components

Truss Qualification/Acceptance Tests

- Inspections and tests, stowed configuration
  - Visual inspection
  - Physical dimensions
  - Mass properties (weight, center of gravity)
  - Electrical (wiring, insulation, grounding)
- Deployment tests and inspections
  - General electromechanical and structural inspection
  - Correlation of extension versus deployment sensor signal
  - Deployment speed
- Inspections, deployed configuraton
  - Visual inspection
  - Physical dimension
- Performance tests
  - Alignment
  - Static load test (stiffness/compliance, strength)

- Environmental tests
  - Vibration (sine, random)
  - Thermal (launch restraint release, hot and cold)
  - Thermal vacuum (inoperational, operational, hot and cold)
- Life test

SECTION 8
RECOMMENDATIONS

The analyses and design studies of Pactruss have shown that it is a viable alternative for constructing the primary Space Station structure. However, its advantages are less apparent when combined with a multiple launch scenario for establishing the structure. The salient points are as follows:

- The principal advantage offered by Pactruss is its ability to put a large amount of truss structure in space at one time.
- A proper study is needed that would capitalize on that advantage.
  - Appropriate flight manifests
  - Resource rearrangement
  - More intricate structure
  - Reduce first flight EVA
- Example: Pactruss should be fitted with a pre-integrated, pre-tested wiring harness with connectors for the modules mounted thereon. Stiff power buses and fluid lines could be installed after deployment.

One possible configuration is shown in Figure 16. The entire primary structure and those facilities necessary for its flight maintenance until the next launch are contained in the first payload. Deployment would be carried out while attached to the Shuttle as is shown in Figures 17 and 18.

The packaged Pactruss would occupy one half of the Shuttle cargo bay and be moved into deployment position as is shown in Figure 19.

This is only one of many alternatives that are available to the Pactruss concept. More study should be undertaken.

REFERENCES

1. von Roos, A., and J. M. Hedgepeth, "Design, Model Fabrication, and Analysis for a Four-Longeron, Synchronously Deployable, Double-Fold Beam Concept; Final Report," Astro Document No. AAC-TN-1139, 20 March 1985.

2. Hedgepeth, J. M., "Application of Pactruss to Space Station Structure, Test 4: Final Report," Astro Document No. AAC-TN-1143, 18 September 1985.

3. Hedgepeth, J. M., and R. R. Miller, "Effect of Member-Length Imperfections on the Deformations and Loads in an Isogrid-Truss Structure," Astro Document No. ARC-R-1012, 1 April 1980.

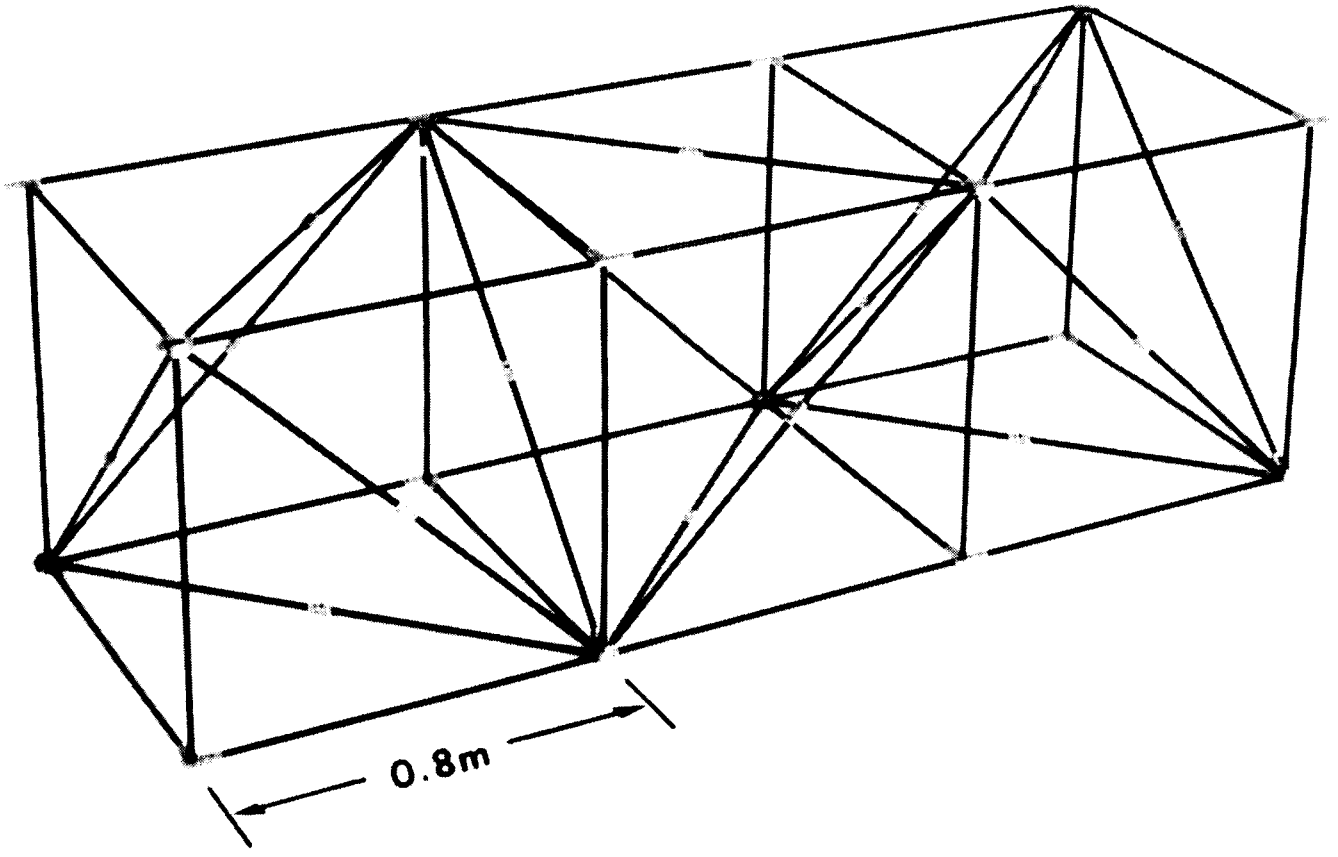

Figure 1. Pactruss beam structure model.

Figure 2. Pactruss area structure conceptual model.

86-1175

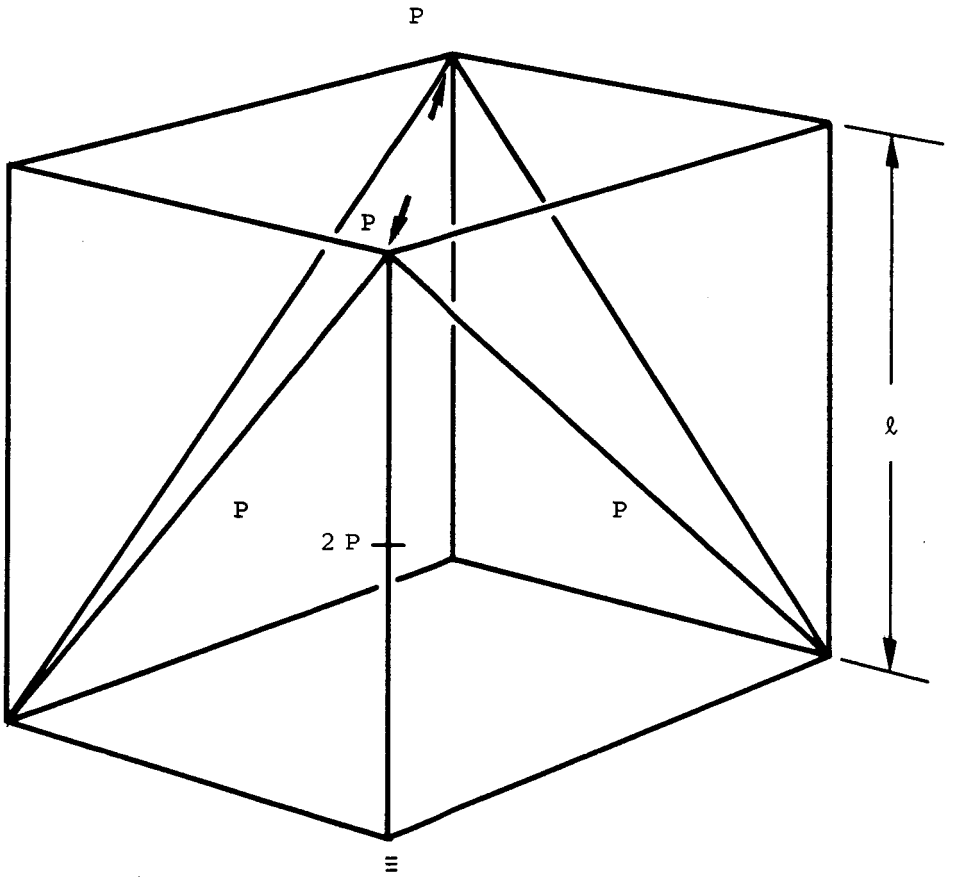

Figure 3. Cube truss geometry and loading.

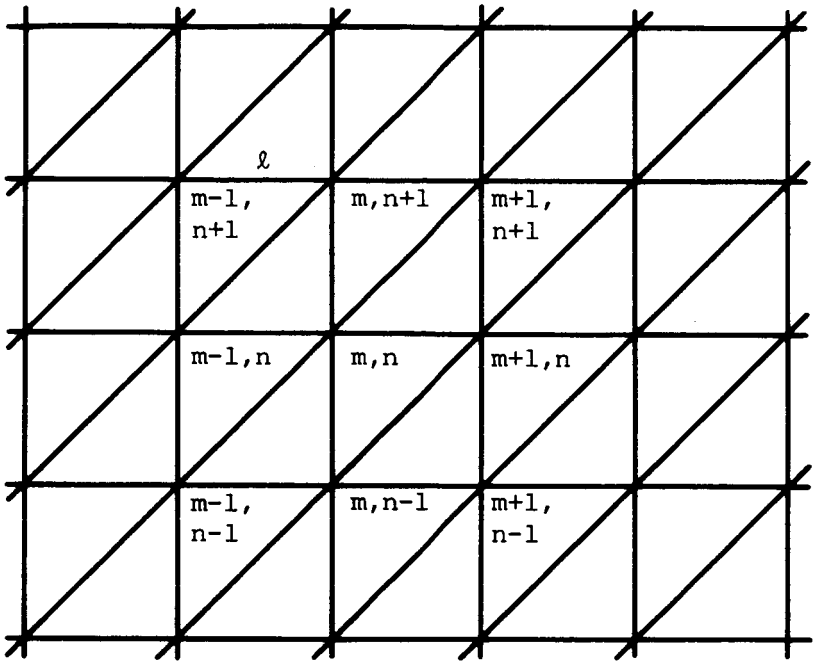

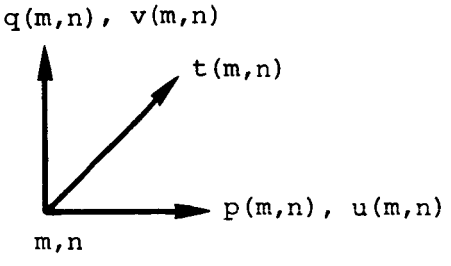

Figure 4. Square lattice geometry and notations for nodes and loads (parallel diagonals).

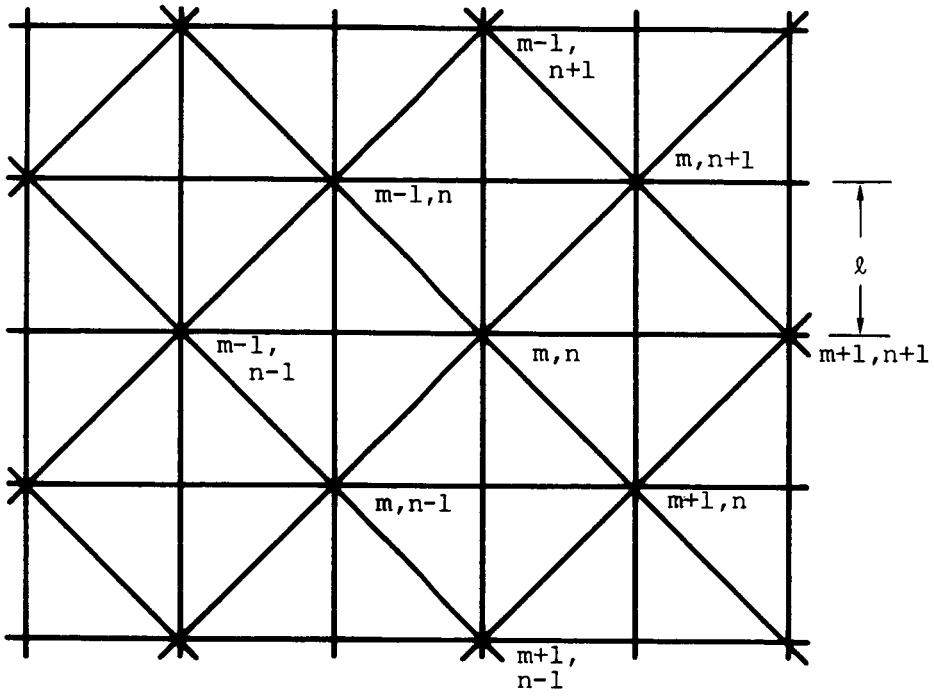

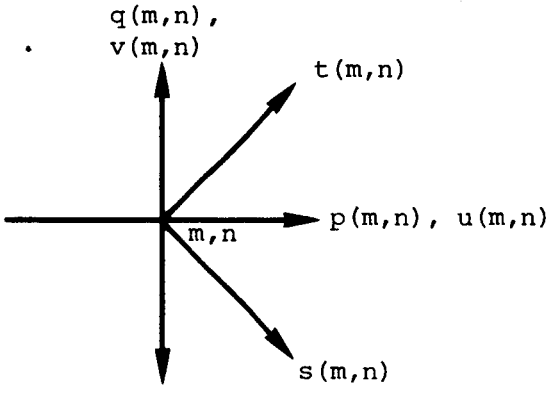

Figure 5. Square lattice geometry and notations for nodes and loads (diamond diagonals).

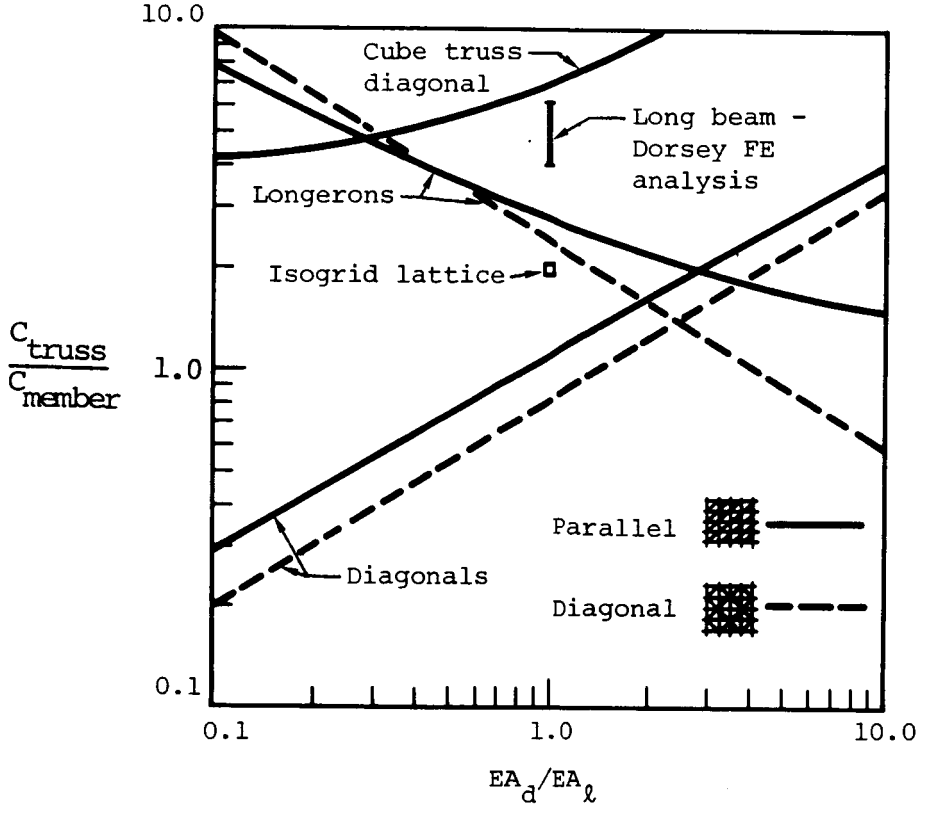

Figure 6. Compliance of surrounding truss structure.

86-1179

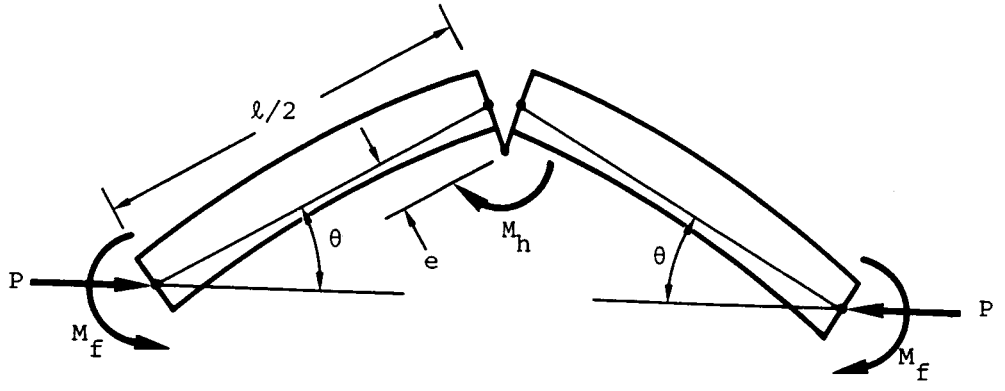

Figure 7. Deploying diagonal member.

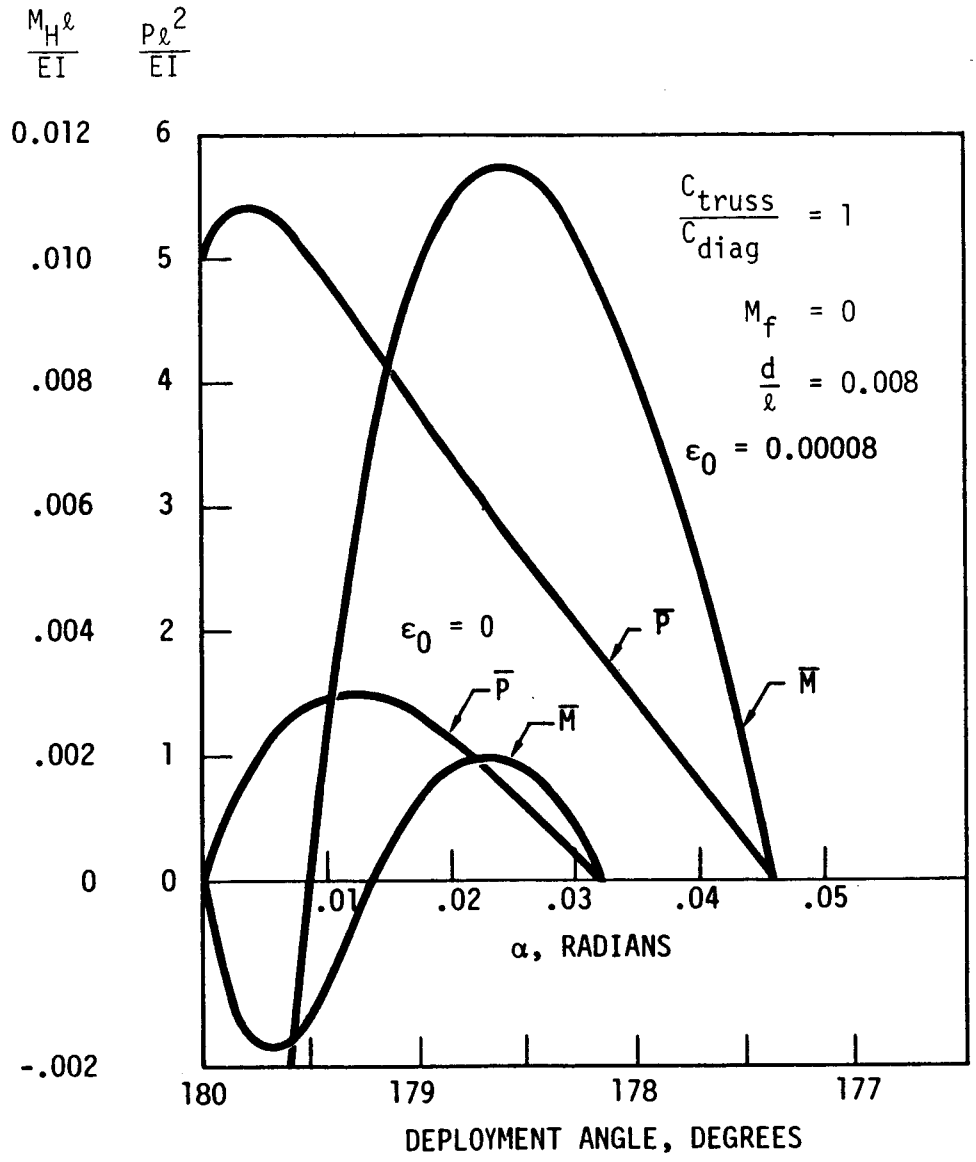

Figure 8. Compressive load and hinge moment for nearly deployed diagonal.

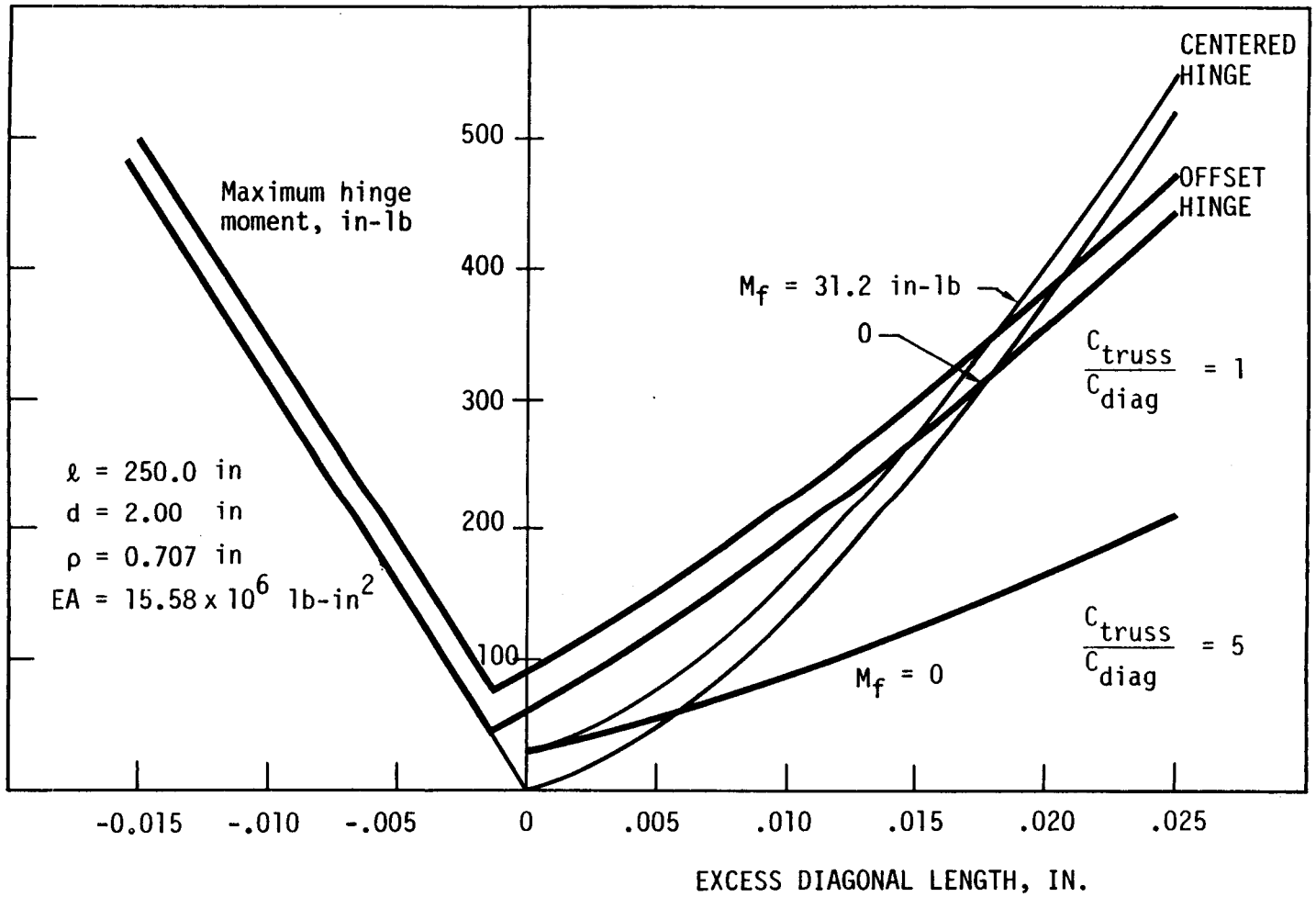

Figure 9. Maximum required central hinge moment to ensure full deployment.

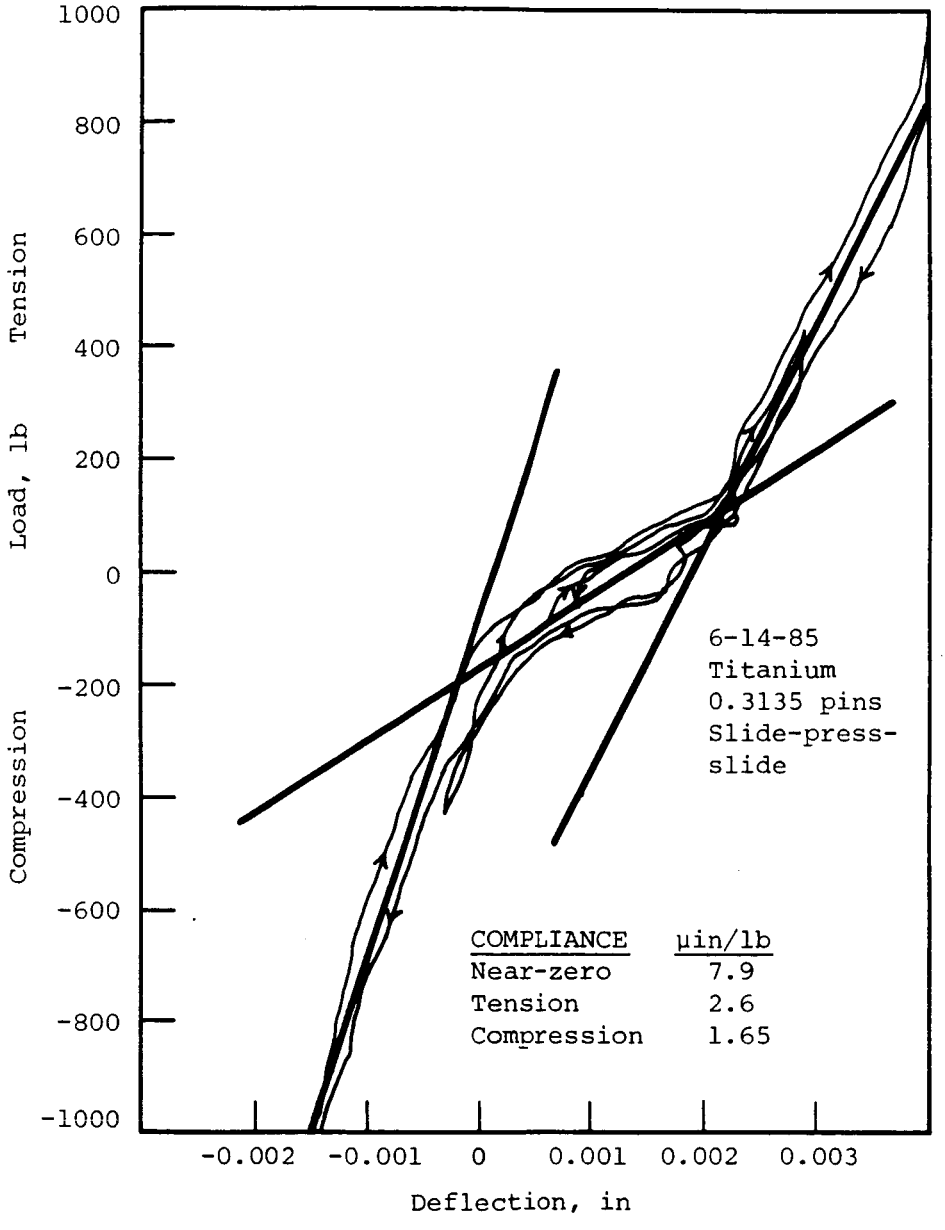

Figure 10(a). Slip-fit pin, experimental load-deflection curves.

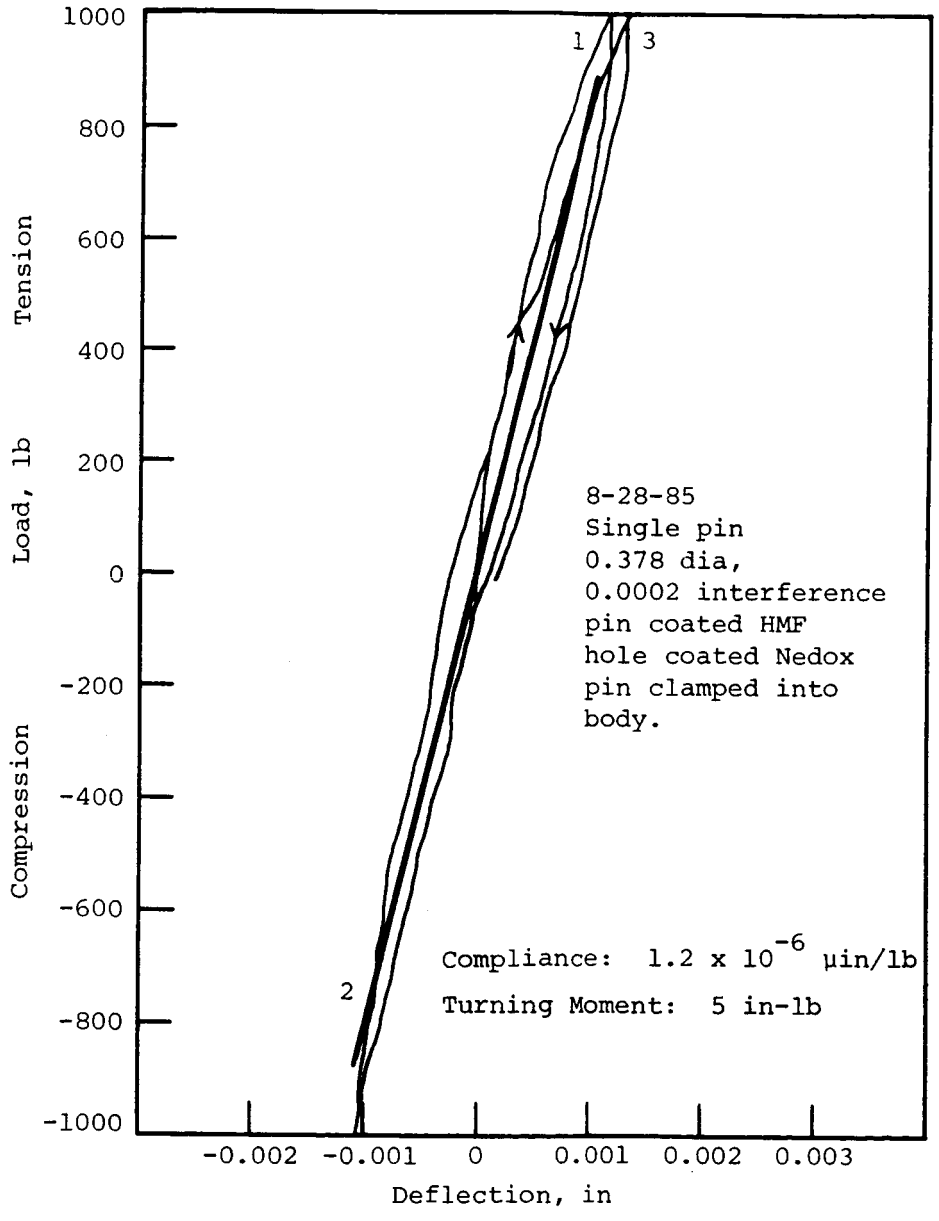

Figure 10(b). Interference fit pin, experimental load-deflection curve.

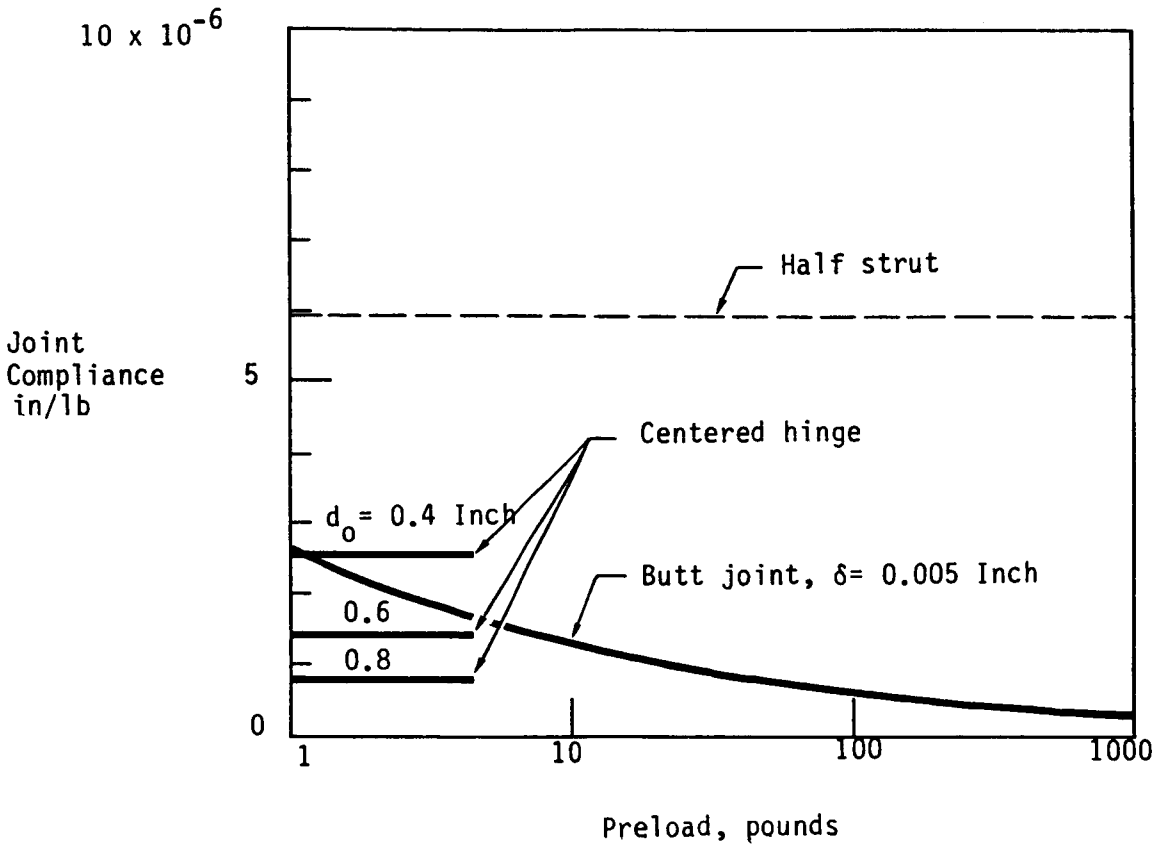

Figure 11. Compliance of hinge and butt joints.

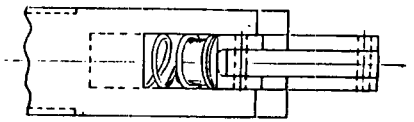

TOP VIEW

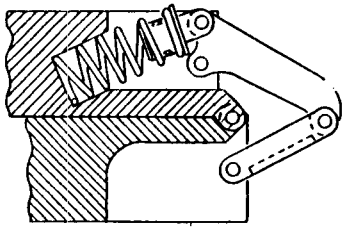

SECTIONED SIDE VIEW (PACKAGED)

(a) SINGLE STAGE LATCH

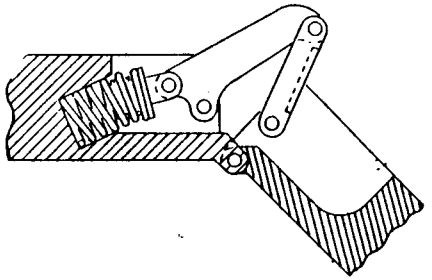

75% DEPLOYED

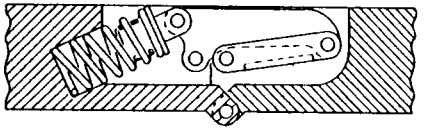

FULLY DEPLOYED

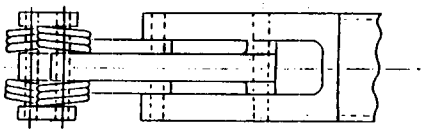

TOP VIEW

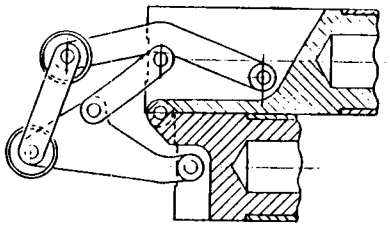

SECTIONED SIDE VIEW (PACKAGED)

(b) TWO STAGE LATCH

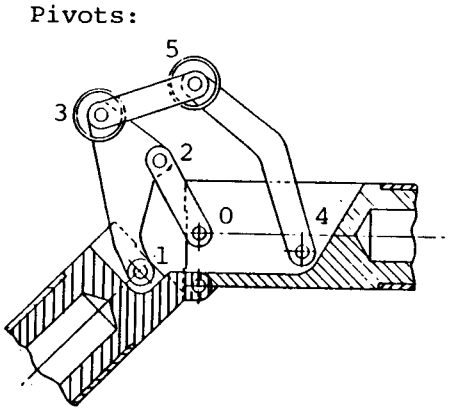

75% DEPLOYED

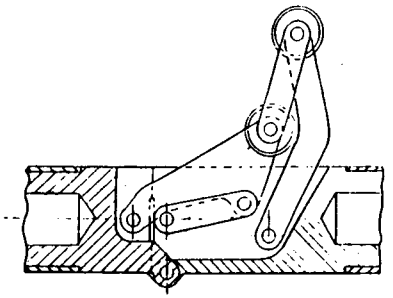

FULLY DEPLOYED

Figure 12. Mid-diagonal hinge designs.

86-1182

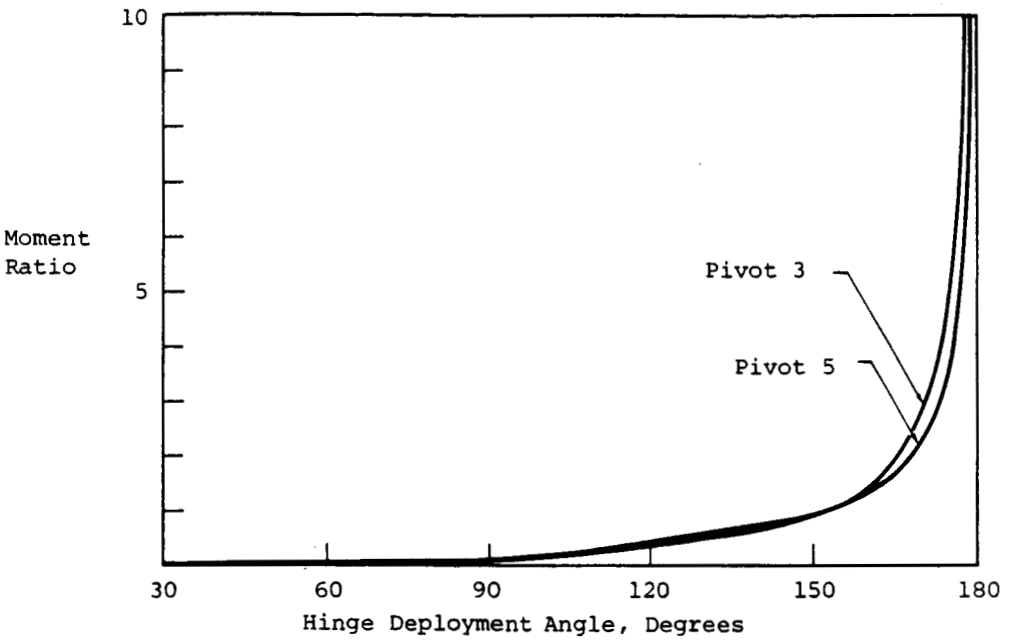

Figure 13(a). Ratio of hinge moment to pivot moment for baseline two-stage latch. Entire deployment range.

85-822

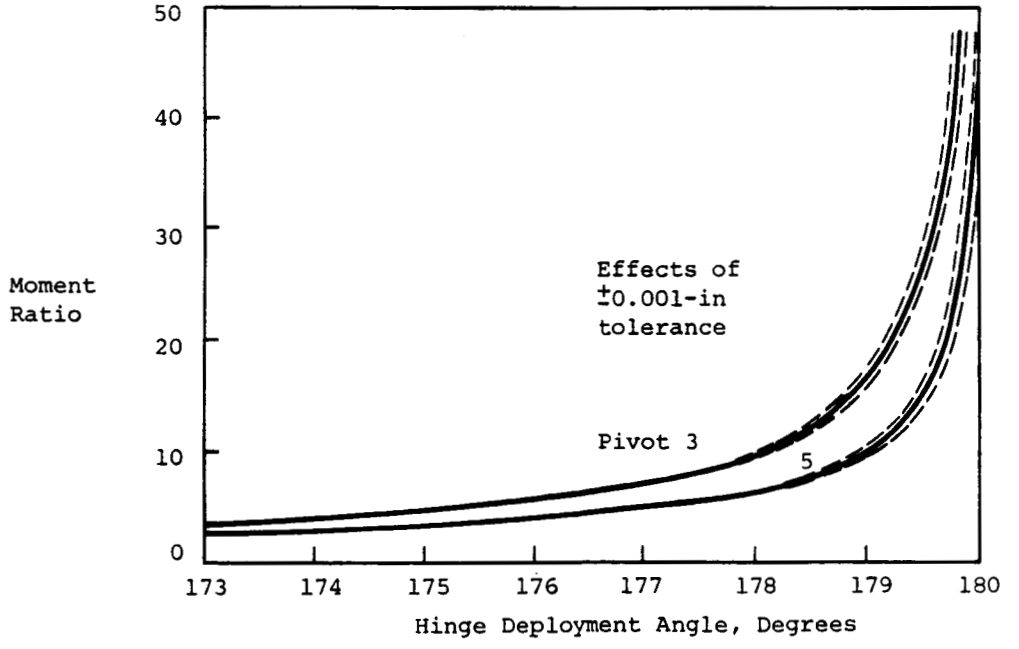

Figure 13(b). Ratio of hinge moment to pivot moment for baseline two-stage latch. End of deployment.

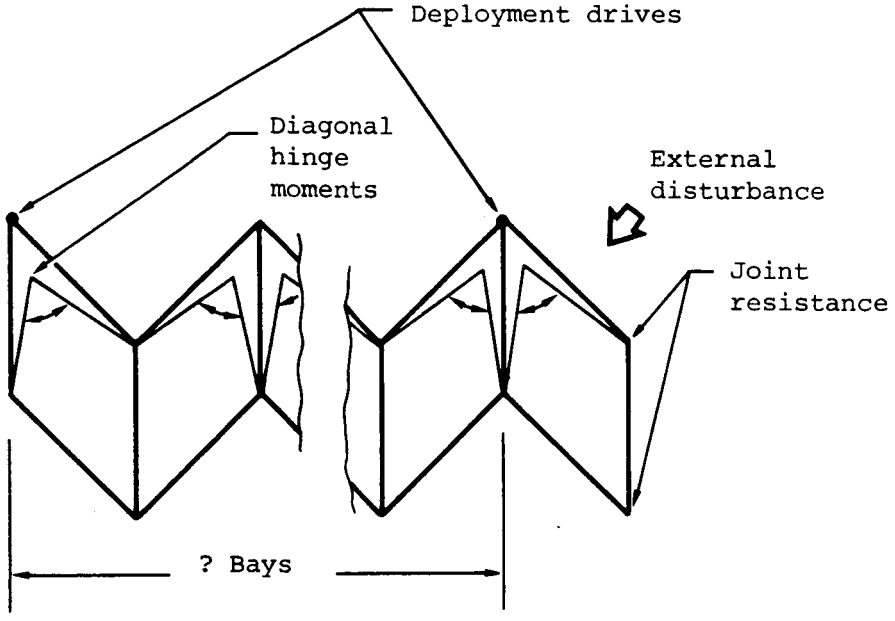

Figure 14. Pactruss deployment reliability factors and concerns.

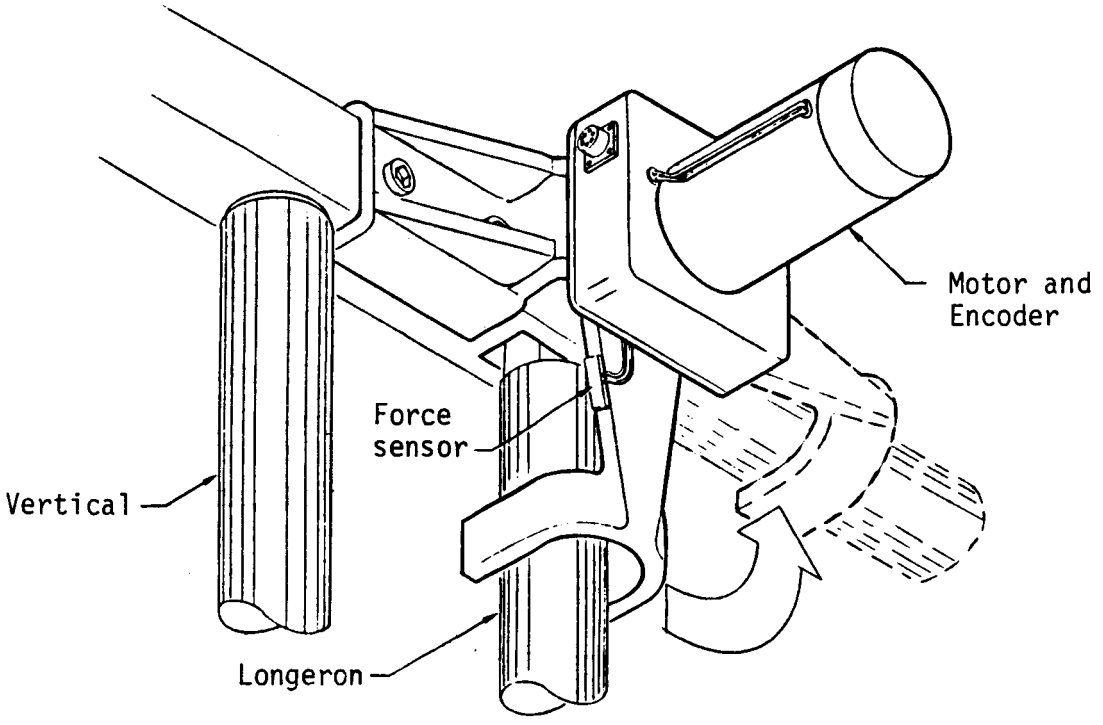

Figure 15. Deployment drive module.

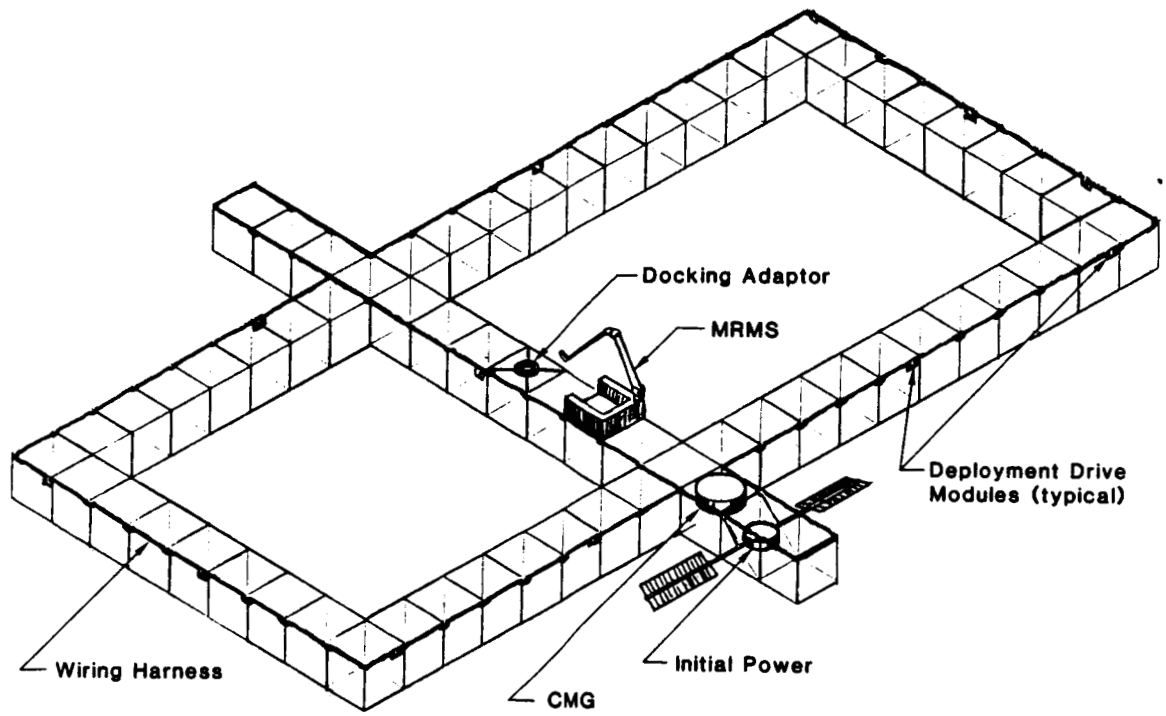

Figure 16. Pactruss space station after flight one.

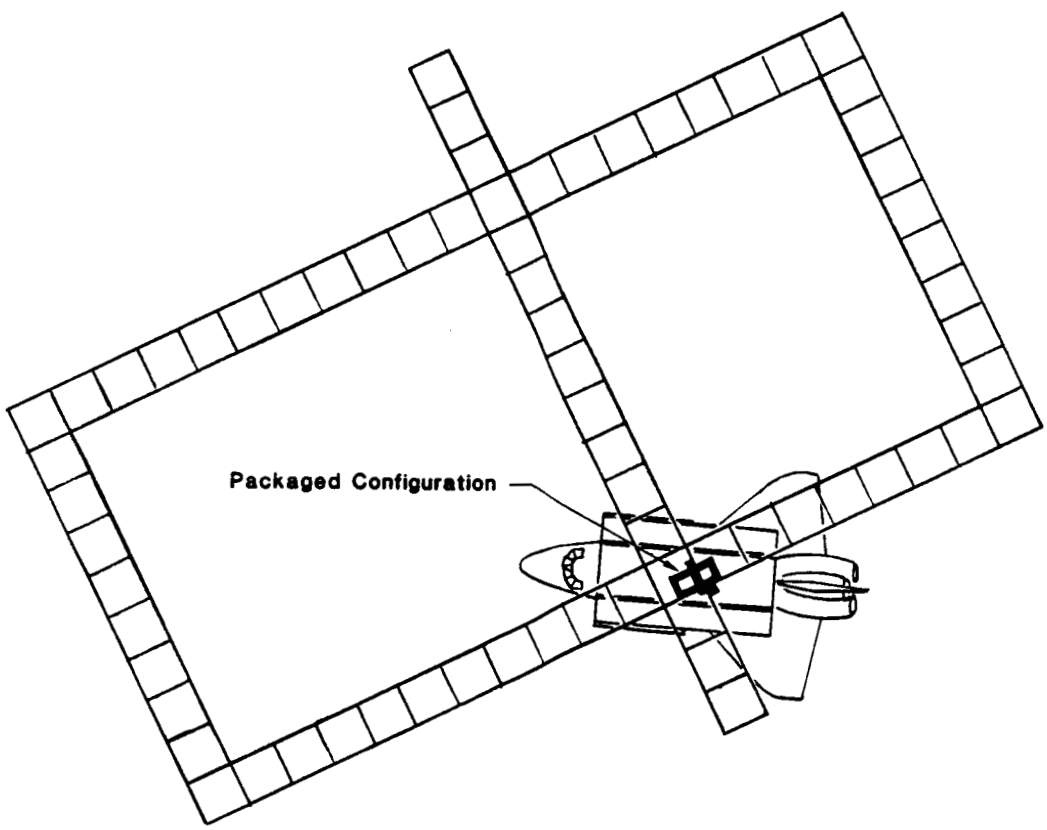

Figure 17. Deployed Pactruss on Shuttle.

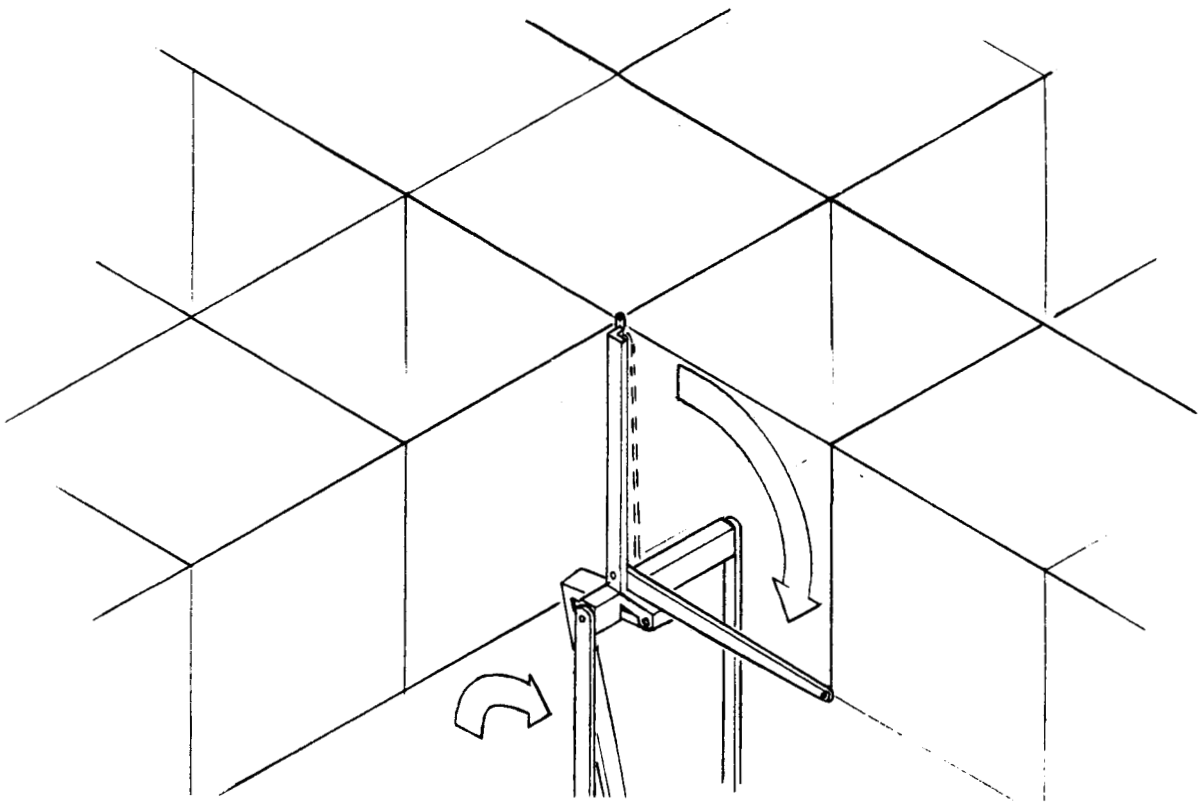

Figure 18. Pactruss/Shuttle attachment.

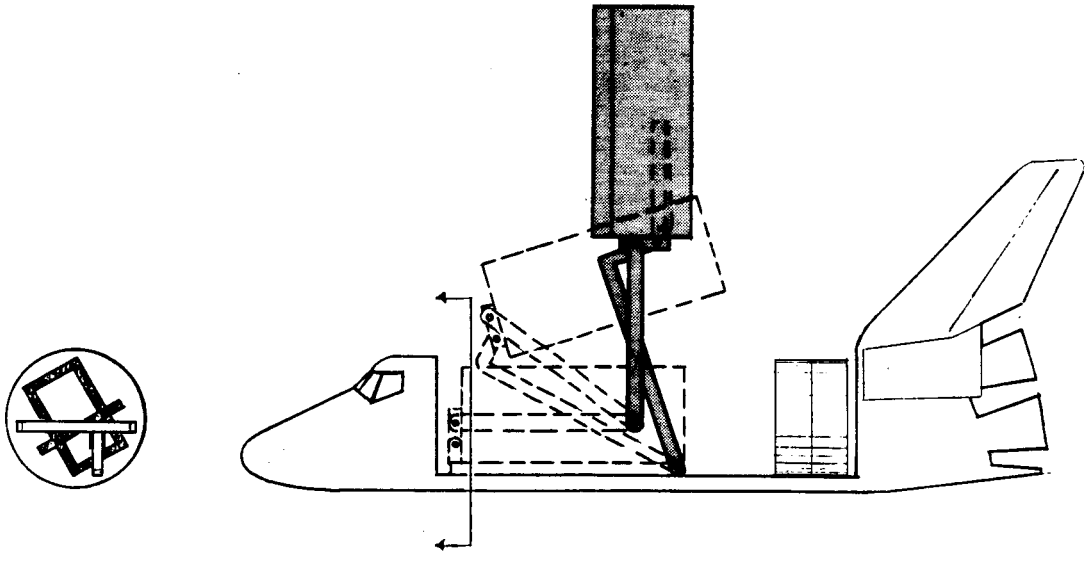

Figure 19. Initial Pactruss deployment.

APPENDIX A

KINEMATICS OF TWO-STAGE LATCH

A computer program written in C
and results for the design geometries
discussed in the text follow.

```
/* LATCH.C-- Calculation of geometry and loading in a two-stage almost-
                over-center latch.  Output shows the joint rotations and moment
                ratios at the various hinge points versus the deployment hinge
                angle.  The design geometry is read from the previously
                prepared ascii file LATCH.DTA.  Also read is the value of
                length tolerance, which is then applied in a worst-case way.
                THIS VERSION APPLIES TO SECOND-STAGE ATTACHMENT TO LINK "12".
                                jmh 9/12/85     */


#include "math.h"

double xy0[6][2],xy[6][2],len[5],phi[6],m_ratio[6],alfa;
int prnt = 1;

main(count,argv)
int count;
char *argv[];
{
    int i,j,n,file;
    char s[50];
    double temp0,temp1,temp2,theta,x,y,*p;
    double eps = .0001;
    double tolerance;

    if(count > 1) eps = atof(argv[1]);

    file = fopen("latch.dta","r");
    for (i=0; i<6; i++) {
        for(j=0; j<2; j++) {
            if((n=fscanf(file,"%F",&xy0[i][j])) != 1) {
                printf("\n\tLATCH.DTA file corrupt!!!\n");
                exit();
            }
        xy[i][j] = xy0[i][j];
        }
    }

    if((n=fscanf(file,"%F",&tolerance)) != 1) {
        printf("\n\tLATCH.DTA file corrupt!!!\n");
        exit();
    }
    temp1 = xy0[2][0]-xy0[0][0];
    temp2 = xy0[2][1]-xy0[0][1];
    len[0] = sqrt(temp1*temp1+temp2*temp2);
    len[0] += tolerance;

    temp1 = xy0[2][0]-xy0[1][0];
    temp2 = xy0[2][1]-xy0[1][1];
    len[1] = sqrt(temp1*temp1+temp2*temp2);
    len[1] -= tolerance;

    temp1 = xy0[3][0]-xy0[1][0];
    temp2 = xy0[3][1]-xy0[1][1];
    len[2] = sqrt(temp1*temp1+temp2*temp2);
    len[2] += tolerance;

    temp1 = xy0[5][0]-xy0[3][0];
    temp2 = xy0[5][1]-xy0[3][1];
    len[3] = sqrt(temp1*temp1+temp2*temp2);
```

```
    len[3] += tolerance;

    temp1 = xy0[5][0]-xy0[4][0];
    temp2 = xy0[5][1]-xy0[4][1];
    len[4] = sqrt(temp1*temp1+temp2*temp2);
    len[4] -= tolerance;

    alfa = atan((xy0[3][1]-xy0[1][1])/(xy0[3][0]-xy0[1][0]))
                        - atan((xy0[2][1]-xy0[1][1])/(xy0[2][0]-xy0[1][0]));

    xy0[1][0] += tolerance;

    newpoints(0.);

    quest_out();

    prt_header();

    for(n=0; n<5; n++) {
        theta = .1*n;
        if(newpoints(theta)==-1) {
            printf("\n\tAborted.  Second-stage geometry is bad.");
            fprintf(prnt,"\f");
            exit();
        }
        moments(theta,eps);
        prt_results(theta);
    }
    for(n=1; n<=10; n++) {
        theta = .5*n;
        if(newpoints(theta)==-1) {
            printf("\n\tAborted.  Second-stage geometry is bad.");
            fprintf(prnt,"\f");
            exit();
        }
        moments(theta,eps);
        prt_results(theta);
    }
    for(n=1; n<=18; n++) {
        theta = 10*n;
        if(newpoints(theta)==-1) {
            printf("\n\tAborted.  Second-stage geometry is bad.");
            fprintf(prnt,"\f");
            exit();
        }
        moments(theta,eps);
        prt_results(theta);
    }
    fprintf(prnt,"\n\t\tPivot coordinates of packaged latch:\n");
    prt_coords();
    fprintf(prnt,"\f");
}

int quest_out()
{
    int chr;

    printf("\n\tDo you want the output directed to LST:? (Y/N) <N> ");
    if(((chr=getchar()) == 'Y') || (chr == 'y')) {
        prnt = open("lst:",1);
```

```
        printf("\n\tMake sure that printer is ready.\n");
    }
}


prt_header()
{
    double *p;

    fprintf(prnt,"\n\n\n\t\t\tDEPLOYING TWO-STAGE LATCH\n\n");
    fprintf(prnt,"\t\tPivot coordinates of deployed latch:\n");

    prt_coords();

    fprintf(prnt,"\n\n\tHinge Angle\tPhi0\tPhi1\tPhi2\tPhi3\tPhi4\tPhi5\n");
    fprintf(prnt,"\t\t\t   Mh/M0   Mh/M1   Mh/M2   Mh/M3   Mh/M4   Mh/M5\n\n");
}


prt_coords()
{
    double *p = xy;

    fprintf(prnt,"\tx0,y0 = %6.3f,%6.3f",*p,*(p+1));
    fprintf(prnt,"\tx1,y1 = %6.3f,%6.3f",*(p+2),*(p+3));
    fprintf(prnt,"\tx2,y2 = %6.3f,%6.3f\n",*(p+4),*(p+5));
    fprintf(prnt,"\tx3,y3 = %6.3f,%6.3f",*(p+6),*(p+7));
    fprintf(prnt,"\tx4,y4 = %6.3f,%6.3f",*(p+8),*(p+9));
    fprintf(prnt,"\tx5,y5 = %6.3f,%6.3f",*(p+10),*(p+11));
}

prt_results(theta)
double theta;
{
    int i,j;
    double *p;

    fprintf(prnt,"\t%8.1f     ",theta);

    p = phi;
    for(i=0; i<6; i++) fprintf(prnt,"%8.2f",*p++);

    fprintf(prnt,"\n\t\t\t");

    p = m_ratio;
    for(i=0; i<6; i++) fprintf(prnt,"%8.3f",*p++);

    fprintf(prnt,"\n\n");
}

int newpoints(theta)
double theta;
{
    int i,j,n;
    double x,y,temp0,temp1,temp2,*ptr,cth,sth,lngth;

    theta *= pi/180.;
    cth =cos(theta);
    sth = sin(theta);
```

```
    x = xy0[1][0];
    y = xy0[1][1];
    xy[1][0] = x*cth - y*sth;
    xy[1][1] = x*sth + y*cth;
    x = xy[0][0] - xy[1][0];
    y = xy[0][1] - xy[1][1];
    lngth = sqrt(x*x+y*y);
    temp0 = atan2(y,x);
    temp1 = acos((-len[1]*len[1]+len[0]*len[0]+lngth*lngth)/2./lngth/len[0]);
    temp2 = acos((-len[0]*len[0]+len[1]*len[1]+lngth*lngth)/2./lngth/len[1]);
    phi[0] = pi + temp0 -temp1;
    phi[1] = temp2 + temp0 - theta;
    phi[2] = pi - temp1 - temp2;
    temp0 = phi[1] + theta + alfa;

    xy[2][0] = xy[0][0] + len[0] * cos(phi[0]);
    xy[2][1] = xy[0][1] + len[0] * sin(phi[0]);
    xy[3][0] = xy[1][0] + len[2] * cos(temp0);
    xy[3][1] = xy[1][1] + len[2] * sin(temp0);

    x = xy[3][0] - xy[4][0];        /* Note: xy[4][j]=xy0[4][j] */
    y = xy[3][1] - xy[4][1];
    lngth = sqrt(x*x + y*y);

    if((lngth < (len[4]-len[3])) || (lngth > (len[3]+len[4]))) return -1;

    temp0 = atan2(y,-x);
    temp1 = acos(-(len[4]*len[4]-len[3]*len[3]-lngth*lngth)/2./lngth/len[3]);
    temp2 = acos(-(len[3]*len[3]-len[4]*len[4]-lngth*lngth)/2./lngth/len[4]);
    phi[3] = pi - temp1 + temp0 + phi[1] + theta + alfa;
    phi[4] = temp2 + temp0;
    phi[5] = pi - temp1 - temp2;

    xy[5][0] = xy[4][0] - len[4] * cos(phi[4]);
    xy[5][1] = xy[4][1] + len[4] * sin(phi[4]);

    for(n=0; n<6; n++) {
        phi[n] *= 180./pi;  /* Convert to degrees   */
    }
    return 1;
}


moments(theta,eps)
double eps,theta;
{
    double temp,xysav[6][2];
    int i,j;

    for(i=0; i<6; i++) {
        m_ratio[i] = phi[i];
        for(j=0; j<2; j++) {
            xysav[i][j] = xy[i][j];
        }
    }
    theta += eps;
    newpoints(theta);

    for(i=0; i<6; i++) {
        temp = phi[i] -m_ratio[i];
```

```
        phi[i] = m_ratio[i];
        m_ratio[i] = temp/eps;
        for(j=0; j<2; j++) {
            xy[i][j] = xysav[i][j];
        }
    }
}
```

DEPLOYING TWO-STAGE LATCH

Pivot coordinates of deployed latch:

x0, y0 = 0.000, 1.000 x1, y1 = -0.600, 1.000 x2, y2 = 1.500, 1.300
x3, y3 = 2.000, 2.700 x4, y4 = 2.000, 0.700 x5, y5 = 2.500, 4.500

Hinge Angle	Phi0	Phi1	Phi2	Phi3	Phi4	Phi5
	Mh/M0	Mh/M1	Mh/M2	Mh/M3	Mh/M4	Mh/M5
0.0	11.31	8.13	3.18	138.70	97.50	8.03
	12.666	8.333	3.333	90.802	34.152	47.318
0.1	12.52	8.92	3.50	145.75	99.94	11.74
	11.582	7.543	3.039	56.731	17.956	30.233
0.2	13.63	9.64	3.79	150.66	101.38	14.38
	10.744	6.931	2.813	42.923	11.652	23.341
0.3	14.67	10.31	4.06	154.53	102.36	16.50
	10.071	6.438	2.633	35.037	8.197	19.403
0.4	15.65	10.93	4.32	157.76	103.07	18.31
	9.514	6.029	2.484	29.830	6.005	16.796
0.5	16.58	11.52	4.56	160.54	103.59	19.89
	9.043	5.683	2.360	26.095	4.494	14.918
1.0	20.66	14.04	5.62	170.79	104.78	25.92
	7.442	4.501	1.941	16.502	0.968	10.033
1.5	24.12	16.10	6.53	177.88	104.90	30.34
	6.480	3.784	1.697	12.326	-0.305	7.847
2.0	27.19	17.86	7.33	183.40	104.58	33.92
	5.817	3.285	1.532	9.943	-0.909	6.567
2.5	29.97	19.40	8.07	187.96	104.04	36.97
	5.322	2.910	1.412	8.387	-1.233	5.710
3.0	32.53	20.78	8.75	191.86	103.37	39.67
	4.932	2.613	1.320	7.283	-1.419	5.090
3.5	34.91	22.02	9.39	195.29	102.63	42.09
	4.615	2.369	1.246	6.455	-1.528	4.614
4.0	37.15	23.15	10.00	198.35	101.85	44.30
	4.350	2.164	1.186	5.809	-1.592	4.236
4.5	39.27	24.19	10.58	201.12	101.04	46.34
	4.124	1.988	1.136	5.288	-1.626	3.926
5.0	41.28	25.15	11.14	203.65	100.23	48.23
	3.927	1.834	1.093	4.859	-1.642	3.667
10.0	57.61	31.70	15.91	221.56	92.28	62.54
	2.780	0.921	0.859	2.727	-1.494	2.300

20.0	80.27	36.71	23.56	241.16	79.30	80.11
	1.898	0.199	0.698	1.447	-1.131	1.378
30.0	97.10	36.95	30.15	252.88	69.17	91.71
	1.510	-0.116	0.626	0.956	-0.912	0.984
40.0	111.01	34.86	36.15	261.00	60.81	100.29
	1.289	-0.286	0.576	0.689	-0.771	0.746
50.0	123.14	31.45	41.69	266.97	53.63	106.85
	1.146	-0.387	0.534	0.517	-0.670	0.574
60.0	134.06	27.24	46.82	271.49	47.33	111.87
	1.043	-0.450	0.493	0.392	-0.592	0.433
70.0	144.08	22.54	51.54	274.90	41.74	115.57
	0.963	-0.488	0.451	0.295	-0.527	0.310
80.0	153.37	17.54	55.83	277.46	36.75	118.12
	0.896	-0.509	0.406	0.219	-0.472	0.200
90.0	162.03	12.39	59.64	279.33	32.28	119.62
	0.837	-0.520	0.357	0.158	-0.424	0.102
100.0	170.13	7.18	62.96	280.66	28.24	120.20
	0.783	-0.521	0.305	0.111	-0.383	0.016
110.0	177.70	1.98	65.72	281.60	24.59	119.98
	0.732	-0.517	0.248	0.078	-0.349	-0.056
120.0	184.77	-3.14	67.91	282.26	21.24	119.11
	0.681	-0.507	0.188	0.057	-0.320	-0.116
130.0	191.33	-8.15	69.48	282.77	18.16	117.71
	0.632	-0.494	0.125	0.047	-0.297	-0.163
140.0	197.40	-13.00	70.40	283.22	15.29	115.89
	0.582	-0.477	0.060	0.045	-0.278	-0.200
150.0	202.98	-17.69	70.67	283.68	12.58	113.74
	0.534	-0.460	-0.006	0.048	-0.263	-0.228
160.0	208.08	-22.20	70.28	284.21	10.01	111.34
	0.486	-0.442	-0.073	0.056	-0.251	-0.251
170.0	212.69	-26.53	69.22	284.81	7.56	108.74
	0.438	-0.424	-0.138	0.066	-0.240	-0.270
180.0	216.84	-30.69	67.53	285.52	5.20	105.96
	0.392	-0.408	-0.200	0.075	-0.231	-0.285

Pivot coordinates of packaged latch:

x0,y0 = 0.000, 1.000 x1,y1 = 0.600,-1.000 x2,y2 = -1.224, 0.083
x3,y3 = -2.491,-0.695 x4,y4 = 2.000, 0.700 x5,y5 = -1.817, 1.048

DEPLOYING TWO-STAGE LATCH

Pivot coordinates of deployed latch:

x0,y0 = 0.000, 1.000 x1,y1 = -0.599, 1.000 x2,y2 = 1.497, 1.318
x3,y3 = 1.987, 2.722 x4,y4 = 2.000, 0.700 x5,y5 = 2.620, 4.481

Hinge Angle	Phi0	Phi1	Phi2	Phi3	Phi4	Phi5
	Mh/M0	Mh/M1	Mh/M2	Mh/M3	Mh/M4	Mh/M5
0.0	11.97	8.61	3.36	143.44	99.31	10.47
	12.022	7.872	3.149	66.043	22.287	34.884
0.1	13.13	9.36	3.66	148.99	101.05	13.43
	11.090	7.192	2.898	47.438	13.651	25.595
0.2	14.20	10.06	3.94	153.21	102.18	15.73
	10.353	6.652	2.701	37.785	9.353	20.780
0.3	15.20	10.70	4.20	156.67	102.97	17.65
	9.750	6.210	2.540	31.705	6.754	17.741
0.4	16.15	11.30	4.45	159.61	103.56	19.31
	9.245	5.838	2.406	27.467	5.014	15.615
0.5	17.05	11.87	4.68	162.20	103.99	20.79
	8.813	5.520	2.292	24.320	3.771	14.029
1.0	21.05	14.33	5.72	171.90	104.98	26.55
	7.317	4.413	1.904	15.840	0.731	9.696
1.5	24.46	16.35	6.61	178.76	105.02	30.84
	6.399	3.727	1.672	11.973	-0.419	7.665
2.0	27.49	18.09	7.41	184.14	104.65	34.35
	5.759	3.245	1.514	9.722	-0.974	6.451
2.5	30.25	19.61	8.13	188.60	104.08	37.36
	5.277	2.879	1.398	8.234	-1.275	5.630
3.0	32.79	20.98	8.81	192.44	103.40	40.02
	4.897	2.589	1.309	7.170	-1.448	5.030
3.5	35.16	22.21	9.45	195.82	102.65	42.41
	4.586	2.349	1.237	6.368	-1.549	4.568
4.0	37.38	23.33	10.05	198.84	101.86	44.60
	4.326	2.148	1.178	5.739	-1.607	4.199
4.5	39.49	24.36	10.63	201.58	101.05	46.62
	4.103	1.974	1.129	5.231	-1.638	3.896
5.0	41.49	25.31	11.18	204.08	100.22	48.50
	3.909	1.822	1.087	4.811	-1.652	3.641
10.0	57.77	31.83	15.94	221.87	92.25	62.74
	2.773	0.916	0.857	2.713	-1.496	2.292

20.0	80.38	36.81	23.57	241.38	79.27	80.26
	1.894	0.197	0.697	1.442	-1.131	1.376
30.0	97.18	37.03	30.15	253.07	69.14	91.85
	1.508	-0.117	0.625	0.954	-0.912	0.983
40.0	111.07	34.93	36.14	261.17	60.78	100.41
	1.288	-0.287	0.576	0.688	-0.771	0.746
50.0	123.19	31.51	41.68	267.13	53.60	106.97
	1.145	-0.388	0.533	0.516	-0.670	0.574
60.0	134.10	27.29	46.81	271.63	47.31	111.99
	1.042	-0.450	0.493	0.391	-0.592	0.433
70.0	144.11	22.58	51.53	275.04	41.72	115.69
	0.962	-0.488	0.450	0.295	-0.527	0.310
80.0	153.39	17.58	55.81	277.60	36.73	118.23
	0.896	-0.510	0.406	0.218	-0.472	0.200
90.0	162.05	12.43	59.63	279.46	32.26	119.73
	0.837	-0.520	0.357	0.157	-0.424	0.102
100.0	170.15	7.21	62.94	280.79	28.22	120.31
	0.783	-0.522	0.305	0.111	-0.383	0.016
110.0	177.72	2.01	65.71	281.72	24.57	120.10
	0.731	-0.517	0.248	0.078	-0.349	-0.056
120.0	184.78	-3.11	67.90	282.39	21.23	119.22
	0.681	-0.507	0.188	0.057	-0.320	-0.116
130.0	191.35	-8.12	69.47	282.89	18.15	117.82
	0.632	-0.494	0.125	0.046	-0.297	-0.163
140.0	197.42	-12.98	70.40	283.34	15.27	116.00
	0.582	-0.478	0.060	0.044	-0.278	-0.200
150.0	203.00	-17.67	70.67	283.80	12.57	113.85
	0.534	-0.460	-0.006	0.048	-0.263	-0.229
160.0	208.09	-22.18	70.27	284.32	10.00	111.45
	0.486	-0.442	-0.072	0.056	-0.251	-0.251
170.0	212.71	-26.51	69.23	284.92	7.55	108.84
	0.438	-0.424	-0.137	0.065	-0.240	-0.270
180.0	216.86	-30.67	67.54	285.62	5.19	106.06
	0.392	-0.408	-0.200	0.075	-0.231	-0.286

Pivot coordinates of packaged latch:

x0,y0 = 0.000, 1.000 x1,y1 = 0.599,-1.000 x2,y2 = -1.225, 0.082
x3,y3 = -2.493,-0.695 x4,y4 = 2.000, 0.700 x5,y5 = -1.816, 1.047

DEPLOYING TWO-STAGE LATCH

Pivot coordinates of deployed latch:

x0,y0 = 0.000, 1.000 x1,y1 = -0.601, 1.000 x2,y2 = 1.503, 1.281
x3,y3 = 2.013, 2.676 x4,y4 = 2.000, 0.700 x5,y5 = 2.290, 4.523

Hinge Angle	Phi0	Phi1	Phi2	Phi3	Phi4	Phi5
	Mh/M0	Mh/M1	Mh/M2	Mh/M3	Mh/M4	Mh/M5
0.0	10.61	7.62	2.99	131.19	94.34	4.18
	13.437	8.884	3.553	184.623	79.809	94.931
0.1	11.88	8.46	3.33	141.80	98.50	9.69
	12.152	7.949	3.203	72.167	25.254	37.963
0.2	13.05	9.22	3.63	147.74	100.43	12.85
	11.187	7.246	2.941	50.053	14.909	26.898
0.3	14.13	9.91	3.92	152.16	101.65	15.25
	10.428	6.692	2.736	39.295	10.077	21.526
0.4	15.14	10.56	4.18	155.74	102.51	17.23
	9.810	6.239	2.571	32.707	7.235	18.233
0.5	16.09	11.16	4.43	158.77	103.13	18.93
	9.293	5.861	2.433	28.189	5.362	15.966
1.0	20.27	13.74	5.52	169.63	104.56	25.28
	7.575	4.594	1.981	17.229	1.233	10.403
1.5	23.78	15.84	6.44	176.99	104.77	29.82
	6.565	3.843	1.722	12.702	-0.182	8.041
2.0	26.88	17.63	7.26	182.65	104.50	33.48
	5.877	3.327	1.551	10.176	-0.839	6.688
2.5	29.69	19.19	8.00	187.31	103.98	36.59
	5.367	2.941	1.426	8.546	-1.189	5.794
3.0	32.27	20.58	8.69	191.28	103.34	39.31
	4.969	2.637	1.331	7.400	-1.389	5.151
3.5	34.67	21.83	9.34	194.76	102.61	41.76
	4.645	2.389	1.256	6.545	-1.507	4.662
4.0	36.92	22.98	9.95	197.86	101.84	43.99
	4.375	2.181	1.194	5.880	-1.575	4.274
4.5	39.05	24.02	10.53	200.66	101.04	46.05
	4.145	2.002	1.143	5.346	-1.614	3.958
5.0	41.07	24.98	11.09	203.22	100.23	47.96
	3.945	1.846	1.099	4.907	-1.633	3.693
10.0	57.46	31.57	15.89	221.26	92.30	62.34
	2.787	0.926	0.862	2.742	-1.492	2.309

20.0	80.17	36.61	23.55	240.94	79.33	79.95
	1.901	0.201	0.699	1.452	-1.131	1.381
30.0	97.02	36.87	30.15	252.70	69.20	91.58
	1.512	-0.115	0.626	0.959	-0.912	0.985
40.0	110.94	34.79	36.15	260.83	60.83	100.16
	1.291	-0.285	0.576	0.691	-0.771	0.747
50.0	123.09	31.39	41.70	266.82	53.65	106.73
	1.147	-0.387	0.534	0.517	-0.670	0.574
60.0	134.02	27.19	46.83	271.34	47.35	111.75
	1.044	-0.449	0.493	0.392	-0.592	0.433
70.0	144.04	22.49	51.55	274.76	41.77	115.46
	0.964	-0.487	0.451	0.296	-0.527	0.310
80.0	153.34	17.50	55.84	277.32	36.78	118.00
	0.897	-0.509	0.406	0.219	-0.472	0.200
90.0	162.01	12.35	59.66	279.20	32.30	119.50
	0.838	-0.519	0.357	0.158	-0.425	0.102
100.0	170.11	7.14	62.97	280.53	28.26	120.08
	0.784	-0.521	0.305	0.112	-0.384	0.016
110.0	177.69	1.95	65.74	281.47	24.60	119.87
	0.732	-0.516	0.248	0.078	-0.349	-0.056
120.0	184.75	-3.17	67.92	282.14	21.26	119.00
	0.681	-0.507	0.188	0.057	-0.320	-0.115
130.0	191.32	-8.17	69.49	282.66	18.18	117.60
	0.632	-0.493	0.125	0.047	-0.297	-0.163
140.0	197.39	-13.03	70.41	283.11	15.30	115.78
	0.582	-0.477	0.060	0.045	-0.278	-0.199
150.0	202.97	-17.71	70.68	283.57	12.60	113.64
	0.534	-0.460	-0.007	0.049	-0.263	-0.228
160.0	208.06	-22.22	70.28	284.10	10.03	111.24
	0.485	-0.442	-0.073	0.056	-0.251	-0.251
170.0	212.68	-26.55	69.22	284.71	7.57	108.64
	0.438	-0.424	-0.138	0.066	-0.240	-0.269
180.0	216.82	-30.71	67.53	285.42	5.22	105.86
	0.391	-0.408	-0.200	0.076	-0.231	-0.285

Pivot coordinates of packaged latch:

x0,y0 = 0.000, 1.000 x1,y1 = 0.601,-1.000 x2,y2 = -1.224, 0.084
x3,y3 = -2.489,-0.694 x4,y4 = 2.000, 0.700 x5,y5 = -1.818, 1.049

APPENDIX B

TEST PROGRAM FOR SPACE STATION PACTRUSS

TEST PROGRAM FOR SPACE STATION PACTRUSS

1.0 SCOPE

The following sections present brief discussions of the major tests to be perfomed for qualification of the Pactruss proposed as the backbone for the Space Station (see Figures 1 and 2). During a later stage of the program, specific detailed test plans and procedures will be generated/implemented in compliance with specified test levels, agreed test philosophies, etc.

2.0 SUMMARY OF MATERIALS, PARTS AND SUBASSEMBLIES TESTS

2.1 TRUSS MEMBER MATERIAL TESTS

The following tests shall be performed on the graphite/epoxy composite material used for truss members in accordance with AAC-TP-TBD:

- Density, determination of
- Bending strength test
- Stiffness test

2.2 TRUSS COMPONENT TENSION TEST

The purpose of this test is to verify the bond strength between the tubular sections and their joint fittings of longerons, battens, and diagonals. Further details will be incorporated on the pertinent component assembly drawings.

2.3 MOTOR QUALIFICATION/ACCEPTANCE TESTS

Document No. TBD, Motor Test Plan, presents a directive for governing the qualification and acceptance testing activities of the motor supplier.

2.4 ACCEPTANCE TESTING OF OTHER ELECTROMECHANICAL COMPONENTS

Electromechanical components purchased as commercial stock items will have to be especially prepared for space per a procurement or process specification. The components will be dismantled, inspected, cleaned, and relubricated per this specification prior to testing.

After space preparation, all components will be subjected to batch screening consisting of vibration testing and thermal cycling. The vibration levels will be the acceptance levels experienced on the Pactruss as determined by analysis. Thermal cycling will consist of five cycles (-65 to +125°C excursions) with functional parameter tests at high and low temperatures. A complete operations screening test to ensure that the components conform to specification will be performed after thermal and vibrational tests are finished.

3.0 QUALIFICATION/ACCEPTANCE TESTING

The qualification/acceptance model Pactruss shall be subjected to the following test in order to verify compliance with agreed equipment specifications.

3.1 INSPECTIONS AND TEST ON STOWED PACTRUSS

Note: Some or all of these tests may be repeated after performance of function and/or environmental tests.

3.1.1 General Visual Inspection

Purpose:

- This inspection is conducted to check the completed workmanship and integrity of the stowed Pactruss and peripheral components with respect to machining, finishes, cabling, cable attachment, bonding, riveting, lubrication, thermal conductive materials, motor mounting, locking and release devices, and limit switches.
- The inspection verifies identification of the truss and its components.

3.1.2 Physical Dimensions Measurement

Purpose:

- To verify conformance of the stowed Pactruss configuration with dimensional specifications (envelope and mounting interfaces).

3.1.3 Mass Properties

Purpose:

- The complete Pactruss will be weighed to verify conformance with specifications.
- To determine the center of mass coordinates for the stowed Pactruss by multiple-scale weighing.

3.1.4 Electrical

Purpose:

- To verify electrical wiring compliance with schematic.
- To measure the electrical resistance between those ground planes and circuit elements of the Pactruss which are designed to be mutually isolated.
- To assure grounding paths, surface resistance, and electrical continuity where specified.

3.2 INSPECTIONS ON DEPLOYED PACTRUSS

These tests may be repeated after or between functional and/or environmental tests.

3.2.1 Visual Inspection

Purpose:

- This inspection is conduted to check those areas of the Pactruss which are inaccessible in the stowed configuration. Inspection is for workmanship and/or integrity of the Pactruss and its components as in 3.1.1. Special scrutiny is to be applied to cables and their attachment after repeated deployments.
- After deployments, the condition of the diagonal mid-span hinges needs to be verified as completely locked.

3.2.2 Physical Dimensions Measurement

Purpose:

- To verify the Pactruss configuration in the deployed condition with the requirements (overall dimensions and interfaces).

3.3 FUNCTIONAL DEPLOYMENT TESTS

Part or all of these tests may be repeated after performance and/or environmental tests.

3.3.1 General Electromechanical and Structural Inspection

Purpose:

- This inspection is conducted to check the general structural integrity and overall electromechanical operation of the complete Pactruss assembly.

Test Conditions, Facilities, Apparatus:

- Ambient room temperature, pressure, humidity
- Horizontal facility equipped either with air bearings, or overhead suspension for zero-gravity simulation
- Mounting means
- Motor switch box
- Test instruments, strain gages, timer

Procedure:

- Position the stowed Pactruss at one end of the test facility and secure in test position via mounting means.
- Release the launch restraint(s), measure and record pertinent parameters, such as time, power, or the force required.
- Connect deployment motor control box, electronic recording instruments, and power source.
- Activate recording instruments.
- Activate deployment mechanism/actuator.
- Record current, voltage, strain in selected truss members.

- Observe the mechanics of deployment.
- Check proper operation of limit switches.
- Record time of extension.
- Subsequent to limit switch arrest of deployment, inspect per 3.1.1.
- Initiate retraction per special procedure.
- Record current if electromechanically retracted.
- Observe the mechanics of retraction and operation of limit switches as applicable.

3.3.2 Correlation of Extension vs. Deployment Sensor Signal

Purpose:

- To calibrate and correlate the deployment sensor signal with the amount of truss extension.

Test Conditions, Facilities, Apparatus:

- Ambient room temperature, pressure, humidity
- Horizontal facility equipped either with air bearings, or overhead suspension for zero-gravity simulation
- Mounting means
- Motor switch box
- Test instruments, strain gages, timer

Procedure:

- Position the stowed Pactruss at one end of the test facility and secure in test position via mounting means.
- Release the launch restraint(s), measure and record pertinent parameters, such as time, power, or the force required.
- Connect deployment motor control box, electronic recording instruments, and power source.
- Activate recording instruments.
- Connect measuring and recording equipment to deployment sensor.
- Activate deployment mechanism/actuator.

- Record current, voltage, strain in selected truss members.
- Deploy the Pactruss intermittently over successive intervals of extension. Record the magnitudes of extension and the corresponding signal of the deployment sensor up to and including limit switch arrest.
- Observe the mechanics of deployment.
- Check proper operation of limit switches.
- Record time of extension.
- Subsequent to limit switch arrest of deployment, inspect per 3.3.1.
- Initiate retraction per special procedure.
- Record current if electromechanically retracted.
- Observe the mechanics of retraction and operation of limit switches as applicable.

3.3.3 Deployment Speed

Purpose:

- To verify deployment speed conformance with specification if power supply voltage varies over a wide range or if functional tests cannot be performed with continuous extension.

Test Conditions, Facilities, Apparatus:

- Ambient room temperature, pressure, humidity
- Horizontal facility equipped either with air bearings, or overhead suspension for zero-gravity simulation
- Mounting means
- Motor switch box
- Test instruments, strain gages, timer

Procedure:

- Position the stowed Pactruss at one end of the test facility and secure in test position via mounting means.
- Release the launch restraint(s), measure and record pertinent parameters, such as time, power, or the force required.

- Connect deployment motor control box, electronic recording instruments, power source, and voltage setting of power supply may be varied.
- Activate recording instruments.
- Activate deployment mechanism/actuator.
- Record current, voltage, strain in selected truss members.
- Observe the mechanics of deployment.
- Check proper operation of limit switches.
- Record time of extension.
- Subsequent to limit switch arrest of deployment, inspect per 3.3.1.
- Initiate retraction per special procedure.
- Record current if electromechanically retracted.
- Observe the mechanics of retraction and operation of limit switches as applicable.

3.4 PERFORMANCE TEST

3.4.1 Alignment Tests

Purpose:

- To verify that alignment and straightness of the fully deployed Pactruss conform to specification.

  Note: The requirement of enormously large test facilities may render this test unfeasible.

Test Conditions, Facilities, Apparatus:

- Ambient room temperature, pressure, humidity
- Horizontal facility equipped either with air bearings, or overhead suspension for zero-gravity simulation
- Mounting means
- Motor switch box
- Test instruments, such as transits, optical targets, laser

Procedure:

- Measure tip deflections and rotation of interface areas of deployed Pactruss in horizontal plane.
- Rotate truss 90 degrees and repeat deflection/rotation measurements.

3.4.2 Static Load Tests

Purpose:

- To verify that structural characteristics of the fully deployed Pactruss conform to specifications, i.e., backlash, compliance (bending, torsional) and strength.

Test Conditions, Facilities, Apparatus:

- Ambient room temperature, pressure, humidity
- Horizontal facility equipped either with air bearings, or overhead suspension for zero-gravity simulation
- Mounting means
- Motor switch box
- Test instruments such as load cells, strain gages, optical targets, transit

Procedure:

- Apply lateral forces, bending moments, and axial torque to structure in increments up to specified levels (including safety factors) and measure deflections and strains. Observe structure for structural instability.

3.5 ENVIRONMENTAL TESTING

3.5.1 Environmental Testing

Purpose:

- To provide controlled exposure of the stowed Pactruss to vibration environments encompassing frequencies and amplitudes representative of STS launch.

Test Conditions, Facilities, Apparatus:

- Ambient room temperature, pressure, humidity

- A special test laboratory with facilities and instrumentation in compliance with the specification will be employed to meet this requirement

Procedure:

- The stowed Pactruss will be attached to a test fixture representing the mounting interfaces of the STS Orbiter. The fixtures will be rigidly attached to the vibration drive(s).
- Triaxis accelerometers will be mounted on the vibration drive, and selected locations on the Pactruss to monitor vibration inputs and responses.
- Order of test will be as follows:
  a. Vibration survey of text fixture for calibration purposes
  b. Low level sine sweep of Pactruss
  c. Acceptance level sine sweep of Pactruss
  d. Qualification level sine sweep of Pactruss (qualification and model only)
  e. Acceptance level random endurance of Pactruss
  f. Qualification level random endurance of Pactruss (qualification model only)
  g. All sine and random vibration inputs to any given axis will be completed and a minimal extension/retraction performed before moving to the next axis

3.5.2 Thermal Tests

Purpose:

- To verify the functional performance requirements of launch restraint release. This test is only performed if launch restraints are released by means different from pyrotechnics.

Facilities and Apparatus:

- Tests will be conducted at a special test laboratory equipped with a thermal chamber and chamber instrumentation
- Motor switch box
- Mounting fixture

- Means for releasing the launch restraints and applying additional release force if required
- Video recording equipment

Procedure:

- Lower the Pactruss temperature to -50°C in a dry atmosphere environment (to prevent condensation).
- Actuate release mechanism.
- Return chamber to ambient and reset the launch restraint.
- Raise the Pactruss temperature to +70°C.
- Actuate release mechanism.

3.5.3 Thermal Vacuum Tests (Qualification Only)

Purpose:

- To verify functional performance characteristics against specified operational requirements at qualification levels of temperature/ pressure

Facilities and Apparatus:

- These tests will be conducted at a special test laboratory equipped with instrumentation and thermal vacuum facilities appropriate to the specification
- Motor switch box
- Means for securing test item in best attitude and counterbalancing weight
- Circuit for applying power to the pyrotechnic release mechanism (if applicable)

Procedure:

- The Pactruss will be exposed to a thermal vacuum test cycle consisting of the following at 10^{-5} torr (or less) pressure:
  - Low temperature survival (-60°C)
  - Low temperature operation (-45°C), launch restraint release one minimal partial deployment retraction
  - Ambient temperature (+23°C)

- High temperature operation (+70°C), one minimal partial deployment/retraction

- High temperature survival (+90°C)

- Thermal cycling (from -45 to +70°C), number of cycles, TBD

3.6 LIFE TESTING

(Performed on qualification model only)

Purpose:

- This series of tests shall comply with the requirement to demonstrate a total truss cycle life capability of TBD cycles. This shall be accomplished by performing TBD (minus cycles to date) deployment/ retraction cycles.

Procedure:

- Set up as per Section 3.3.3.

- Inspect the cycled truss every TBD cycles for evidence of wear and degradation.

4.0 TEST SEQUENCE

The envisioned test sequence is shown in the following table. Post refurbishment tests are basically an acceptance test sequence which may have to be expanded depending on the extent of refurbishment, i.e., extent of disassembly and part replacement.

TABLE B-1: SPACE STATION PACTRUSS TEST SEQUENCE FOR QUALIFICATION/ACCEPTANCE

3.1 Inspections and Tests, Stowed Configuration

3.1.1	Visual Inspection
3.1.2	Physical Dimensions
3.1.3	Mass Properties (Weight, CG)
3.1.4	Electrical (Wiring, Insulation, Grounding)

3.2 Inspections, Deployed Configuration

3.2.1	Visual Inspection
3.2.2	Physical Dimensions
3.3.2	Correlation of Extension Versus Deployment Sensor Signal
3.3.3.	Deployment Speed

3.3 Functional Deployment Tests

3.3.1	General Electromechanical and Structural Inspection

3.4 Performance Tests

3.4.1	Alignment
3.4.2	Static Load Tests (Stiffness/Compliance, Strength)*

3.5 Environmental Tests

	Vibration (Sine, Random) 3 Axes: Low Level Sine, Acceptance/ Qualification Level
3.1.1	Visual Inspection, Stowed
3.1.4	Electrical (Insulation, Grounding)
3.3.1/3	Functional Deployment, Speed (Combined)
3.2.1	Visual Inspection, Deployed
3.5.2	Thermal (Launch Restraint Release: Hot and Cold)*
3.5.3	Thermal Vacuum (Inoperational, Operational: Hot and Cold)*
3.1.1	Visual Inspection, Stowed
3.1.4	Electrical (Insulation, Grounding)
3.3.1/3	Functional Deployment, Speed (Combined)
3.2.1	Visual Inspection, Deployed
3.4.1	Alignment
3.4.2	Static Load Test (Stiffness, Compliance)

3.6 Life Test

3.1.1	Visual Inspection, Stowed
3.1.4	Electrical (Insulation, Grounding)
3.3.1/3	Functional Deployment, Speed (Combined)
3.3.2	Correlation Extension vs. Deployment Sensor Signal
3.4.1	Alignment
3.4.2	Static Load Test (Stiffness, Compliance, Strength)*

TABLE B-1: SPACE STATION PACTRUSS TEST SEQUENCE FOR QUALIFICATION/ACCEPTANCE (CONCLUDED)

Refurbishment

3.1.1	Visual Inspection, Stowed
3.1.2	Physical Dimensions
3.1.4	Electrical (Wiring, Insulation, Grounding)
3.3.1	Functional Deployment
3.2.1	Visual Inspection, Deployed
3.2.2	Physical Dimensions
3.3.2	Correlation Extension vs. Deployment Sensor Signal
3.3.3	Deployment Speed
3.4.1	Alignment
3.4.2	Static Load Tests [Stiffness, Compliance, Strength (Acceptance Level)]
3.5.1	Vibration (Random, Acceptance Level)
3.1.1	Visual Inspection, Stowed
3.1.4	Electrical (Insulation, Grounding)
3.3.1/3	Functional Deployment/Speed Combined
3.2.1	Visual Inspection, Deployed
3.4.1	Alignment
3.1.3	Mass Properties (Weight, CG)
3.1.1	Visual Inspection, Final

Standard Bibliographic Page

1. Report No.	2. Government Accession No.	3. Recipient's Catalog No.
NASA CR-178171		

4. Title and Subtitle	5. Report Date
EVALUATION OF PACTRUSS DESIGN CHARACTERISTICS CRITICAL TO SPACE STATION PRIMARY STRUCTURE	20 February 1987
	6. Performing Organization Code
7. Author(s)	8. Performing Organization Report No.
John M. Hedgepeth	AAC-TN-1147, Rev. A
9. Performing Organization Name and Address	10. Work Unit No.
Astro Aerospace Corporation 6384 Via Real Carpinteria, California 93013-2993	11. Contract or Grant No. NAS1-17536, Task 6
12. Sponsoring Agency Name and Address	13. Type of Report and Period Covered
National Aeronautics and Space Administration Langley Research Center Hampton, Virginia 23665	Contractor Report
	14. Sponsoring Agency Code

15. Supplementary Notes

Langley Technical Monitor: Wilbur B. Fichter
Final Report

16. Abstract

Several aspects of the possible application of the Pactruss concept to the primary truss structure of the Space Station are investigated. Estimates are made of the loads and hinge moments in deploying diagonal members as full deployment is approached. Included are the effects of beam columning and compliance of the surrounding structure. Requirements for joint design are suggested and a new two-stage mid-diagonal latching hinge concept is described or analyzed. The problems with providing the experimental and theoretical tools needed for assuring reliable synchronous deployment are discussed and a first attempt at high-fidelity analytical simulation with NASTRAN is described. An alternative construction scenario in which the entire dual-keel truss structure is deployed as a single Shuttle payload is suggested.

17. Key Words (Suggested by Authors(s))	18. Distribution Statement
Deployable Structures, Truss Structures, Space Station Structure, Joint Concepts, Large Space Structures	Unclassified - Unlimited

19. Security Classif.(of this report)	20. Security Classif.(of this page)	21. No. of Pages	22. Price
Unclassified	Unclassified	74	

For sale by the National Technical Information Service, Springfield, Virginia 22161